UPPSALA
UNIVERSITET

EROI of crystalline silicon photovoltaics

variations under different assumptions regarding

manufacturing energy inputs and energy output

Johan Lundin

Abstract

EROI of crystalline silicon photovoltaics – variations under different assumptions regarding manufacturing energy inputs and energy output
Johan Lundin

**Teknisk- naturvetenskaplig fakultet
UTH-enheten**

Besöksadress:
Ångströmlaboratoriet
Lägerhyddsvägen 1
Hus 4, Plan 0

Postadress:
Box 536
751 21 Uppsala

Telefon:
018 – 471 30 03

Telefax:
018 – 471 30 00

Hemsida:
http://www.teknat.uu.se/student

Installed photovoltaic nameplate power have been growing rapidly around the world in the last few years. But how much energy is returned to society (i.e. net energy) by this technology, and which factors contribute the most to the amount of energy returned? The objective of this thesis was to examine the importance of certain inputs and outputs along the solar panel production chain and their effect on the energy return on (energy)investment (EROI) for crystalline wafer-based photovoltaics.

A process-chain model was built using publicly available life-cycle inventory (LCI) data sets. This model has been kept simple in order to ensure transparency. Univariate sensitivity analysis for processes and multivariate case studies was then applied to the model.

The results show that photovoltaic EROI values are very sensitive to assumptions regarding location and efficiency. The ability of solar panels to deliver net energy in northern regions of the earth is questionable. Solar cell wafer thickness have a large impact on EROI, with thinner wafers requiring less silicon material. Finding an alternative route for production of solar-grade silicon is also found to be of great importance, as is introduction of kerf loss recycling. Equal system sizes have been found to yield an primary EROI between approximately 5.5-19 depending on location and assumptions. This indicates that a generalized absolute EROI for photovoltaics may be of little use for decision-makers. Using the net energy cliff concept in relation to primary EROI found in this thesis shows that primary EROI rarely decreases to less than the threshold of 8:1 in univariate cases. Crystalline photovoltaics under similar system boundaries as those in the thesis model does not necessarily constrain economic growth on an energetic basis.

Sammanfattning

Den totala installerade effekten avseende solpaneler växer mycket fort runt om i världen och har så gjort ett tag. Om den snabba tillväxten av installerad effekt fortsätter kommer möjligen solkraft utgöra en betydande del av världens kraftproduktion inom en relativt snar framtid. Solkraftssystem levererar naturligtvis energi som kommer samhället till gagn, men har även kostat energi att tillverka. *Energy return on investment* (EROI) är en kvot vilken beskriver förhållandet mellan levererad bruttoenergi och energibehovet för detta tillgängliggörande. En låg EROI-kvot innebär att en låg andel energi blir tillgänglig för ekonomisk aktivitet. Detta kan i framtiden innebära begränsningar av vårt levnadssätt. Det är således av vikt att veta vilket energiutbyte som är att vänta utifall solkraft visar sig utgöra en mycket stor del av det framtida globala energisystemet.

Det här examensarbetet syftade till att undersöka i vilken utsträckning de olika energiinkomsterna- och utgifterna för kristallina solpaneler påverkar EROI. Databasen ecoinvent innehåller en stor mängd LCI-dataset för processer och produkter som ingår i produktionskedjan för konventionella solceller. Energidata från dessa dataset användes för att modellera en produktionskedja. De ingående parametrarna och resulterande EROI utsattes sedan för en enklare känslighetsanalys. Vidare har (mer eller mindre) realistiska scenarier konstruerats vilket resulterat i ett EROI-spann.

Resultaten indikerar att de absolut viktigaste EROI-faktorerna är mottagen solinstrålning och paneleffektivitet. Solinstrålning korrelerar starkt med geografisk placering. Placering av solpaneler på nordligare breddgrader riskerar att ge en EROI så låg att tveksamhet uppstår gällande nettoenergileverans. Vidare visade solcellernas tjocklek starkt påverka EROI.

Den utförda scenarioanalysen resulterade i en EROI på mellan 5.5-19. Systemgränserna hölls konstanta men antaganden skiftade. De alla högsta EROI-värdena erhölls i de fall där solpanelernas effektivitet var lika hög som för de i dagsläget allra bästa cellerna samt tjockleken minskat till 100 µm.

När EROI sjunker till under 8:1 blir nettoenergitillskottet till samhället snabbt lågt (det så kallade. nettoenergistupet). Så länge EROI är över 8:1 är även över 90% av levererad energi nettoenergi. EROI för solpaneler befinner sig över 8:1 i de flesta undersökta fallen (med givna systemgränser). Således förefaller inte en hög andel solkraft hämma det ekonomiska systemets tillväxt.

Table of Contents

Abbreviations:

AM – air mass
BoS – balance of system
c-Si – monocrystalline silicon
CED – cumulative energy demand
CVD – chemical vapor deposition
EPBT – energy payback time
EROI – energy return on investment
$EROI_{PE}$ – primary energy return on investment
$EROI_e$ – thermal equivalent energy return on investment
FBR – fluidized bed reactor
GDP – gross domestic product
kW_p – kilowatt-peak nameplate power
LCA – life-cycle assessment
LCI – life-cycle inventory
LCIA – life-cycle impact assessment
LCOE – levelized cost of electric energy
mc-Si – multicrystalline silicon
MG-Si – metallurgical-grade silicon
NEA – net energy analysis
PE – primary energy
PR – performance ratio
PV – photovoltaic
r-Si – ribbon silicon
SiC – silicon carbide
SoG-Si – solar-grade silicon
STC – standard testing conditions
TSI – total solar irradiance
UCTE – Union for the Co-ordination of Transmission of Electricity, association of transmission operators in continental Europe

1 Introduction

Our global society is currently addicted to fossil fuels, our society would not persist in it's current state without these fuels. Our cities is in effect dependent on artificial ecosystem services to allow current population densities, and these services require energy (Odum, 1973). Energy production is as of now the most important use of fossil fuel resources. But one must ask what it is that is really provided by fossil fuels. Is it just energy, or energy with a high degree of availability and utility?

The industrial revolution would not have been possible without the discovery and use of highly available energy resources (i.e. coal, oil and gas). But currently more and more work seems to be required to extract a given amount of oil, and not even increased effort is able to meet increasing demand. It appears as if society's extraction of fossil fuels has depleted the highly available oil stocks according to the *best first principle*. This phenomenon that we now are experiencing is called *peak oil*, meaning that production flow rates of the world's oil fields is either hitting a plateau or are in decline ("World oil supply," n.d.). This is a fate all fossil fuel resource stocks is likely to face. One effect of peak oil/coal/gas is that energy will no longer be as available as it used to be. Our whole society is built around the use of highly available fuel resources. These resources will need replacement if economic growth is to continue and living standards maintained.

One way of decreasing the dependence on fossil fuels is to transition into a society based around renewable energy resources. These resource stocks is renewed by incoming sunlight. Sunlight, although abundant, is a very dilute energy resource with low availability for performing work. Systems which transform sunlight or the associated flowing renewable resources (e.g. water and wind) into useful energy carriers is required. These systems require energy to construct and maintain. Effort is thus required even for renewable energy, which lowers availability to society.

A smooth transition into a renewable society can be achieved if the availability of energy does not decrease substantially. One way to measure the availability of energy from a resource is arguably the *energy return on investment* (EROI). Photovoltaics is often said to be an important part of the renewable energy puzzle. Large-scale development does however require photovoltaic EROI to be sufficiently high. If not, economic growth and/or quality of life will decrease in the long run. EROI for photovoltaics can however fall within a rather large range of values depending on assumptions made. Examining the effects of different assumptions in a clear way may help establish and narrow the range of photovoltaic EROI presented in literature.

2 Goal

The purpose of this thesis is to find to what extent input- and output parameters affect final EROI values for conventional silicon-based (i.e. monocrystalline, polycrystalline and ribbon solutions) photovoltaic cells. The impact of different assumptions regarding production, location and their effect on EROI will also be examined. This is accomplished through a univariate sensitivity analysis and several multivariate cases. Wafer-based cells and modules dominates the market as of 2012 with a market share of approximately 90% justifying the focus on this technology(IEA PVPS Task 1, 2012).

3 Methodology

Calculation of EROI requires knowledge about energy inputs and outputs over any given system's lifetime. The inputs is found through a simplified process-chain analysis regarding silicon's path from metallurgical silicon to PV panel. At each process-step direct or indirect energy inputs enter, either as embodied energy or as actual energy input from within or beyond the system border. There

is for all calculation purposes no difference between direct and indirect energy. A distinction is made in this thesis between EROI as a general expression, EROI$_{PE}$ which uses primary energy units as output and EROI$_e$ meaning output has been treated as straight electric energy/thermal equivalents.

Data for energy and material inputs is taken from Jungbluth et al. (2012) which provides a set of ecoinvent LCI data-sets regarding production of PV panels and associated processes. A r*educed system* is modeled using inputs known to be energy intensive. An *extended system* is also modeled, having the same *cumulative energy demand* (CED) as presented in Jungbluth et al. (2012). Energy inputs are accounted for in primary energy units. The reason for modeling an already assessed system in detail is to gain control over the energy inputs used, thereby facilitating sensitivity analysis without access to LCA software. See chapter 7 for details regarding system modeling.

Sensitivity analysis is performed by changing one parameter at a time according to either a percentage scheme or by using quoted energy requirements for alternative manufacturing routes. Result from the sensitivity analysis will be illustrated by spiderplots and a qualitative assessment. See chapter 8 for details. The variability is illustrated by using a number of cases and scenarios deemed realistic, producing a range of EROI estimates. The work of previous LCA and NEA for photovoltaics are also assessed, notably Prieto and Hall (2013).

3.1   System boundaries and flow diagram

Conventional LCA methodology states that system boundaries are to be set before data collection commences. Limitations on time and resources has forced this rule to be abandoned in favor of adapting system boundaries to the process-chain data found available. Jungbluth et al. (2012) contains a large amount of LCI data-sets from the ecoinvent database.

A process-chain following the silicon flow is modeled in a spreadsheet. This model is a *reduced system* compared to Jungbluth et al. (2012). This provides transparency and a more easy oversight of the system at hand. The "complete" Jungbluth et al. (2012) system is also modeled, keeping the *reduced system core* and adding the difference between the two systems as a "black box". Processes more than one level away from the main silicon flow chain are not considered in the reduced system (e.g. energy requirement for aluminum *production* is included, but not indirect embodied energy requirements for this). Aluminum, steel, copper, glass and concrete are the only considered indirect material inputs in the reduced system. These materials are known to be energy-intensive and/or constitute a large mass fraction of a solar panel.
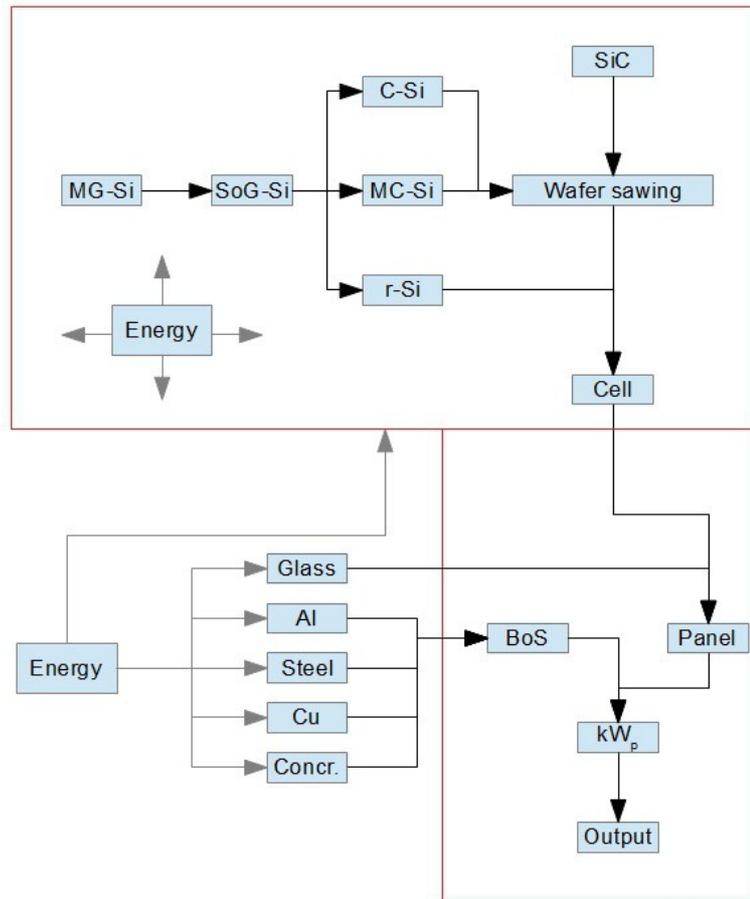
Illustration 1: Flow chart and system boundaries, reduced system

4   LCA, net energy analysis and EROI

Life-cycle assessment (LCA) is a methodology framework for assessing a certain product's impact (e.g. energy demand, greenhouse gas emissions, eutrophication) on the environment and society over it's entire lifetime. Material and energy flows are examined and compiled into a *life-cycle inventory* (LCI).

Rebitzer et al. (2004) published a comprehensive overview of LCA methodology and stress the importance of an appropriate *functional unit*, which is the basis of comparison. This unit may be the physical product or system itself, but is more commonly defined as a service that is provided by aforementioned system or product (e.g. consider the difference between a water pump, and one m^3 of water raised to a height of one meter by the same pump).

 Analysis can be carried out as a process chain-analysis, economic *input/output* (I/O) analysis or as a hybrid method of these two. A complete process-chain analysis can be very time-consuming to perform. Simplification may be necessary, either by reducing the number and level of processes or reducing the number of inputs and outputs of each process. I/O-analysis means that the material and energy flows used in a process-chain analysis is replaced by corresponding financial flows. This financial flow is then multiplied by corresponding energy use or emission for a particular sector per economic unit (e.g. MJ/USD). I/O analysis uses data that is highly aggregated, and allows for much broader system boundaries compared to process-chain analysis.

Rebitzer et al. (2004) also offers a short review of the hybrid methods available. The tiered hybrid method means that (far)-upstream processes that are non-specific are subject to I/O-analysis, other processes closer to point of observation are treated by process-chain analysis. Another hybrid approach is the disaggregation of I/O-tables in order to increase the resolution, ideally approaching process-chain accuracy. Rebitzer et al. states that hybrid methods generally provide better accuracy than just process- or I/O analysis.

The *life-cycle impact assessment* (LCIA) phase may begin once a data-set has been established and system boundaries have been set. LCA software perform these impact assessments according to predefined methods. Such software use either included LCI datasets or external databases (e.g. ecoinvent). LCI data for processes often reference sub-processes and flows, which can be automatically included by modeling software.

An LCI (hopefully) includes all relevant inputs and outputs for a specific functional unit. A flow often relevant is the flow of energy necessary to produce the functional unit of choice. Energy demand is often the cause of pollution (e.g. greenhouse gases, acidification) and is thus included in a LCI. This provides the foundation for a *net energy analysis* (NEA). Net energy analysis is a type of life-cycle assessment that concerns the energy returned to society after energy expenses has been accounted for (Herendeen, 2004). NEA could, according to the author of this thesis, be placed within the LCA framework. The result of a net energy analysis (i.e. data on delivered energy and energy consumption) can then easily be used to find the EROI.
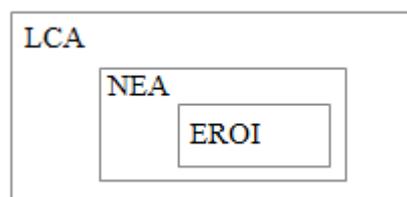
Illustration 2: Relationship between LCA, NEA and EROI

4.1 LCA and photovoltaics

Alsema et al. (2009) have on account of the IEA developed general methodology guidelines for performing a LCA for photovoltaic panels. CED and *energy payback time* (EPBT) are among the indicators to be reported in each LCA according to guidelines. Efficiency and irradiation are also to be reported.

The guidelines proposes a few standard assumptions about technical and performance aspects of a photovoltaic power plant. System lifetime is assumed to be 30 years for all components except inverters which needs to be replaced every 15 years. The irradiation received by the panels should either be set as optimal for any given location (with respect to tilt and orientation) or use actual mean values. Performance degradation over system lifetime should also be included.

The exact method recommended depends on the goal and scope of the assessment, although process-based assessment is favored according to guidelines. Region-wide electric energy mix is to be used, except if production-chain steps are very local and only uses a certain energy source.

System boundaries is recommended to include the panel and all necessary *balance-of-system* (BoS) components. Alsema et al. (2009) further recommends use of kWh delivered electric energy as the functional unit when comparing different PV technologies, while m^2 panel area is appropriate when there is a surface limitation (i.e. environmental impact on a specific building or quantifying possible energy gain on a given surface). It's also possible to use *kilowatt-peak nameplate power* (kW_p) as the functional unit of choice when performing analysis. This thesis will utilize the kW_p.

5 EROI theory

The following chapter will describe some of the key aspects of EROI. Topics include system boundary issues, energy quality corrections, different accounting methods and the connection between energy and economics.

5.1 EROI methodology

EROI can broadly be described as the ratio between energy made available to society through a certain process and the energy cost for this (Hall et al., 2009). The EROI ratio is often expressed as *EROI:1* in text. One way to easily explain EROI is to think of it as a ratio that answers the question: *How many barrels of oil are made available by the use of one barrel of oil in the production process?* This is just an example, the concept itself extends to any energy carrier and source. Murphy et al. (2011) expresses the ratio formally as:

$$EROI \ = \ \frac{E_g}{E_{in}} \ = \ \frac{E_g}{E_c + E_{op} + E_d} \qquad (1)$$

where the subscripts *c*, *op* and *d* represents **c**onstruction, **op**eration and **d**ecommission for a certain process and infrastructure and E_g is the gross energy output. This approach is general and valid for all energy production and energy carrier production systems. Some of this gross energy is then fed back into the energy producing sector. For example: an EROI of 10:1 means society (including the energy sector) have ten units of gross energy available. The production of additional ten marginal energy units requires the input of one unit, which leaves society (excluding energy sector) with nine units of net energy.

It is tempting to interpret EROI as a measure of process chain energy- or conversion efficiency, but this would not be accurate (Hall and Klitgaard, 2012). A process chain or system with a high EROI can still be inefficient at transforming an energy resource into gross energy. EROI for fuels and energy systems should rather be interpreted as a measure of availability of gross energy to society

originating from a given source and/or process.

The amount of net energy returned to society, which essentially means energy available for economic activity outside the energy sector, can according to Murphy et al. (2011) be found by:

$$E_{net} = E_g - \left(E_c + E_{op} + E_d \right) \qquad (2)$$

The amount of energy necessary for gross energy production is subtracted from gross energy produced. Gross energy production could in turn be thought of as an initial energy resource or flow E_0 (for example insolation or barrels of oil in place at a specific site) going through a series of process steps before considered gross energy ready for use. Each process step is associated with a transformation/conversion efficiency resulting in energy losses.

$$E_g = E_0 \cdot (\eta_1 \cdot \eta_2 \cdot \ldots \cdot \eta_n), \eta \leq 1 \qquad (3)$$

By combining eq. (2) with (1) and (3) it is possible to obtain:

$$E_{net} = E_g \cdot \left(1 - \frac{1}{EROI} \right) = E_0 \cdot (\eta_1 \cdot \eta_2 \cdot \ldots \cdot \eta_n) \cdot \left(1 - \frac{1}{EROI} \right) \qquad (4)$$

The amount of net energy returned to society hence depends on (among other things) the resource size, energy resource transformation efficiencies and EROI. Total net energy returned to society can be increased by a) finding more resources, b) improving conversion efficiencies or c) increasing EROI. An EROI of 1:1 means that no net energy will be made available to society from a given process (or the global energy system as a whole), and a EROI of less than one constitutes a net energy sink.

5.2   Inputs, outputs and system boundaries

The general approach to EROI is dividing the gross energy output by the energy expended to gain this gross energy. Energy output data may at a first glance seem easy to find. The energy industry is, after all, all about delivering energy to society. As such the industry should have production data that could easily be disclosed to researchers and the public. This is in general true for producing entities, although the private nature of actors can sometimes be limiting. System boundaries for outputs is generally varied by changing the amount of process steps involved from the mine-mouth and onward. That is, the boundary depends on the distance from the mine-mouth to point of observation (Murphy et al., 2011). For petroleum and natural gas this would mean distance in time and space inside the process chain from the wellhead. A system boundary for flowing renewable energy (e.g. hydro, solar and wind) comparable to mine-mouth/extraction would be electric energy produced at generator/panel level.

Two principal categories constitutes the energy inputs in a process, *direct* and *indirect* energy. According to Bullard et al. (1978) direct energy refers to fuel and electric energy used directly in the production process (e.g. example diesel used for drilling or electric energy used for sawing silica wafers). Direct energy expended in a process can often be found either by direct measurement or by examining the monetary expense for energy attributed to this process and dividing by corresponding energy carrier prices. System boundary issues arise when deciding where processes end. Is, for example, direct energy consumption for lighting and space heating in a production facility part of the production process or should these expenses be left out of the analysis?

Indirect energy is the energy not directly associated with the studied process, or energy crossing the system boundary from the environment (Bullard et al., 1978). The indirect energy category also include *embodied* energy, which is energy used in the manufacture of capital and material inputs. Examples include energy necessary to produce etching chemicals for silica wafers and energy expenses for mining, smelting and casting metals which are made into drill bits or frames. The

embodied energy is often found in an aggregated state for a specific item crossing the system border from the surroundings. The number of indirect energy inputs tend to grow very fast when system boundaries is widened (Bullard et al., 1978). More and more energy also gets embodied in a certain product the further downstream in the manufacturing chain one travels.

An energy system can be visualized by using the *energy circuit language* developed by Howard T. Odum (see Brown (2004) for a comprehensive overview). This language is a set of symbols that represents energy flows (both direct and embodied energy) in a system. *Illustration 3* is a representation of the biophysical economy using the energy circuit language.
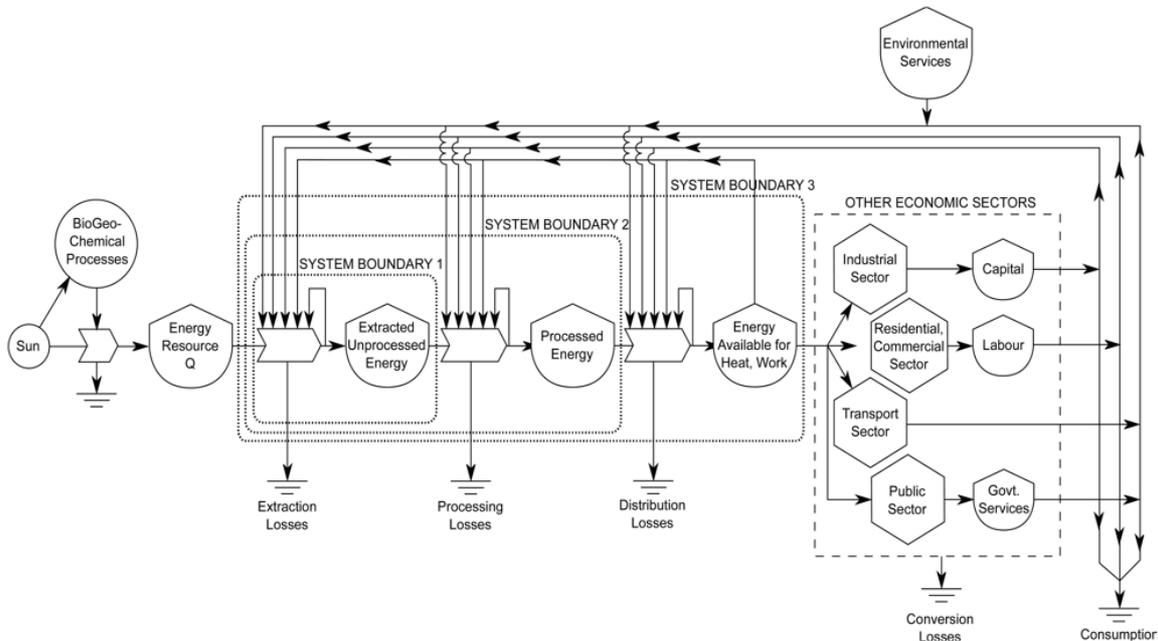
Illustration 3:Biophysical economy, Murphy et al., (2011) adapted from Hall et al., (1986)

Murphy et al. (2011) proposes a collection of EROI indicators, each corresponding to a different set of system boundaries. The framework is two-dimensional; inputs and outputs can be divided into different levels of detail independent of each other. A standard measure ($EROI_{stnd}$) is presented which includes direct, indirect and embodied energy at the energy extraction point.

Mulder and Hagens (2008) presents a framework of similar two-dimensional type, although with different notation, fewer levels of detail and a system boundary that varies according to different criteria (i.e. distance from mine-mouth (Murphy et al., 2011) compared to accounting method of non-energy inputs (Mulder and Hagens, 2008). Second-order EROI calculations within this framework includes both direct and indirect inputs and is said to correspond to established LCA accounting.

The system boundaries of an EROI analysis will heavily influence the outcome. A model including every single possible input and output of a system would obviously give a true value to the system EROI. But as the number of inputs increase, so does the uncertainties. Completeness is connected to uncertainty (Mulder and Hagens, 2008).
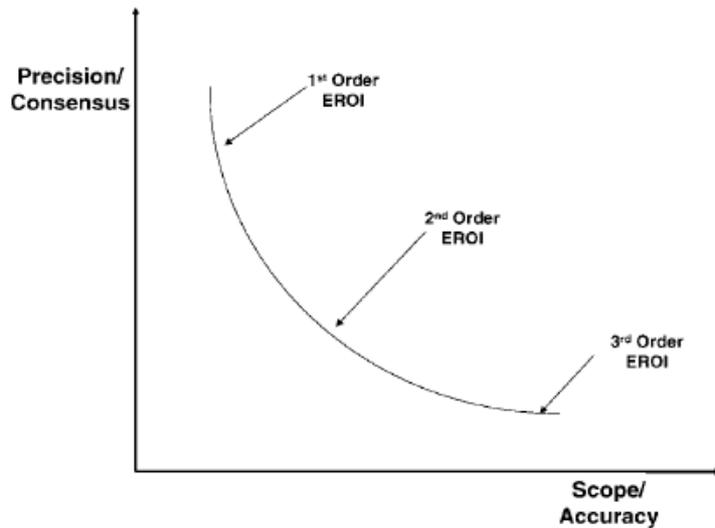
Illustration 4: Conceptual connection between completeness and uncertainty (Mulder and Hagens, 2008)

The observed output of an energy system will ultimately depend on the point of observation and the process transformation efficiencies for getting the initial latent energy resource E_0 to this point. Eq. (3) tells us that fewer process steps considered in an analysis results in larger gross energy output. Few process steps from latent energy resource E_0 to E_g means "small" system boundaries and vice versa. The amount of processes studied also defines where the system boundary for output is drawn (Murphy et al., 2011). Since E_g constitutes the numerator of EROI, a smaller boundary regarding the output will positively influence EROI.

All energy invested can at some point in a global/universal perspective be considered direct input. Energy inputs previously considered indirect and embodied becomes direct inputs as system boundaries are expanded.

The EROI of certain systems can change over time. EROI of oil wells might decrease as pressure drops and more effort is needed per produced barrel. EROI for a particular solar power facility might increase once old panels are replaced by new ones. If these new panels utilize the old infrastructure then the site-specific EROI will increase.

5.3 Energy quality correction

Not all energy is equal, joules carried by different energy carriers differ in quality. A joule of electric energy is generally considered worth more than a joule of heat, and heat joules originating from different energy carriers all have differing utility. One could choose not to make any quality corrections at all, meaning all energy is treated equal. This would, in the case of photovoltaic or hydro power production, mean electric energy output at generator/cell level being compared to energy inputs consisting of both fossil fuel heating values and electric energy.

One way to quality-correct inputs and outputs is to convert all energy into *primary energy* (PE). Primary energy is defined by IEA as "*...the first energy form downstream in the production process for which multiple energy uses are practical*" (IEA, 2012). The primary energy content of fossil and biomass fuels is equal to respective heating values of the resource stock (e.g. crude oil, peat, anthracite). The electric energy delivered by renewable systems utilizing flowing renewable stocks (e.g. hydro-, wind and solar power) is converted straight to primary energy. These flows have no

other energy uses (in our current *energy system*). This is in a sense not a true quality correction since all inputs and outputs, regardless of origin, are seen as primary energy equivalents. It does however take into account the fact that one joule of electric energy produced in an energy system dominated by combustion techniques corresponds to an even larger amount of primary energy joules.

Electric energy input and output can be transformed into primary energy equivalents if the thermal grid efficiency η for a given system (or the electric grid as a whole) is known:

$$E_{PE} = \frac{E_{el}}{\eta} \qquad (5)$$

The result is an energy return on investment with primary energy in the numerator (i.e. $EROI_{PE}$). One could also choose not to calculate displaced primary energy and instead treat output as thermal equivalents resulting in $EROI_e$ (i.e. electrical energy units in numerator).

A true and complete quality correction can be achieved through exergy- or economic-based quality correction according to Murphy et al. (2011). The weighted energy input or output is given by:

$$E_t^* = \sum_{i=1}^{N} \lambda_{i,t} \cdot E_{i,t} \qquad (6)$$

where $\lambda_{i,t}$ is the weighing factor and $E_{i,t}$ is energy.

An economic quality correction assumes that energy-carriers prices accurately reflects the quality of carried thermal units. The price of a fuel is seen as a measure of it's utility in the current economy. A simple way of adding weight to different carriers would be to compare their price to some reference fuel:

$$\lambda_{i,t} = \frac{P_{i,t}}{P_{0,t}} \qquad (7)$$

where $P_{i,t}$ stands for the price of energy carrier *i* at time *t* and $P_{0,t}$ represents the price of the reference energy carrier at time *t*. More complex economic quality-correction methods exists (Divisia-index) which eliminates the need for a reference fuel.

It is also possible to quality-correct energy carriers using an exergy-based method. Exergy is defined as the maximum amount of work a system can perform on it's reference environment as the system approaches equilibrium. The ability to do work is what society is interested in, which also can be seen as the quality of an energy carrier. Rosen (2004) offers an overview on exergy and energy quality.

5.4 **The biophysical economy and EROI**

All economic activities need throughput of energy, and all processes consume exergy content which lead to an increase in entropy (Peet, 2004). The biophysical approach to economy means application of the first- and second law of thermodynamics on economic systems and acknowledging that resources are limited.

This view differs from the classical view of economics, where *capital* is considered the economic system input. Capital is assumed to flow through the system in a circular fashion, amplifying itself so growth can be achieved. This view does not take into account the physical processes that is actually occurring, instead it sees the events inside the economic sphere as separate from those in the physical sphere. Biophysical economics evaluate economic systems on a physical basis primarily. The flow of energy and matter through the economic system is essentially seen as unidirectional and the main cause of growth (Stern, 2011). All energy and material inputs to a real

system will give rise to high-entropy wastes which can not be recycled (be that particle emissions or waste heat). This is a consequence of the second law of thermodynamics which applies universally as far as we know. A limit is thus placed on the economy and it's ability to grow, since low-entropy (high-quality) resources are limited both globally and universally. Some resource stocks (i.e. the sun) are however so large that constraints do not apply in real life. Biophysical economists also argue that substitution possibilities are limited, energy resources cannot be replaced by non-energy capital and vice verse. Energy is needed in order to *produce and use* said capital.

Increasing EROI is subject to decreasing marginal returns. At a certain EROI more than 90% of the energy output is considered net energy. Moving from an EROI of 40:1 to 80:1 does not in any way increase the percentage of net energy returned to society like an increase from 4:1 to 8:1. Further improvement is thus connected to diminishing marginal returns. It has been stated above that economic growth needs net energy to flow and net exergy to be consumed. Economic growth can thus be said to be limited by low EROI, but high EROI does not necessarily cause economic growth.
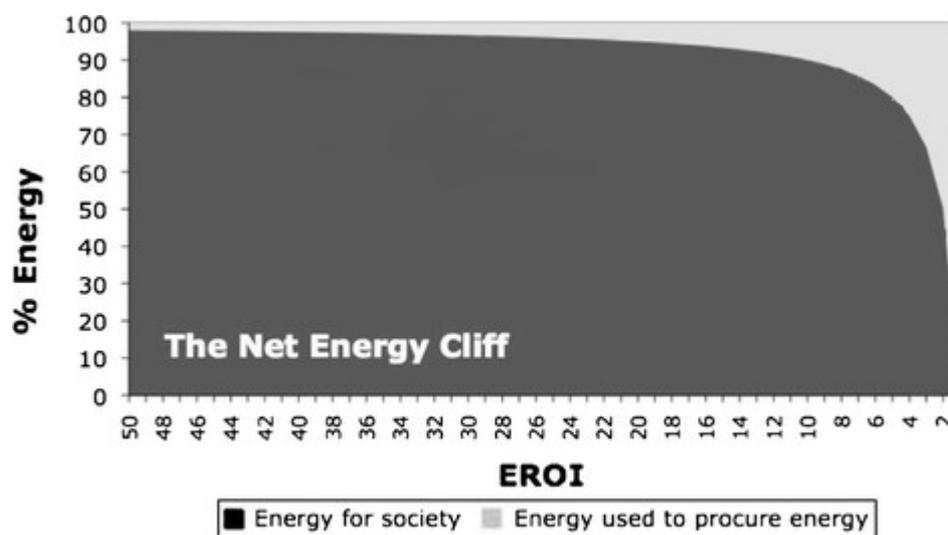
Illustration 5: Net energy cliff, adapted from (Murphy et al., 2010)

5.4.1 GDP and energy, cause and effect

The correlation between energy use and *gross domestic product* (GDP) is high. Correlation does however not imply causation, and there might be other factors driving growth of GDP. Stern (2011) offers an overview on the subject and mentions that production is a function of both capital and labor as well as energy. Causation regarding energy and GDP remains somewhat inconclusive and is dependent upon the time horizon, country and causality test used. Warr and Ayres (2010) find that energy- and exergy use cause GDP growth in the United States while a study by Chiou-Wei et al. (2008) is inconclusive regarding the U.S economy. This implies neutrality. The same study also shows some Asian economies where causality runs from GDP growth to energy consumption. Stern (2011) mentions some studies where energy use have caused GDP growth in the short run, but where GDP growth ends up causing energy consumption in the long run. A *bi-directional* causative state also exists, which is different from a state of inconclusiveness. This state means energy consumption and GDP growth appear to affect each other in a feedback loop.

Causation differ between countries for a number of reasons. This means policies regarding energy efficiency, consumption and greenhouse gas reductions will have different effects, since they all

mean less energy will need to be used. An economy driven by the increased use of fuel will likely shrink if less energy is to be used. Such an economy will also be more affected by the transition to low-EROI energy sources. Economies where economic growth drives energy consumption will on the other hand not be as crippled by such policies or transitions into low-EROI sources. The potentially low EROI for photovoltaics is *not necessarily* a problem, especially when coupled with possible CO_2-reductions and less combustion for power production.

6   Insolation, output and solar cell efficiencies

6.1   Irradiance and insolation

The energy carried by incoming sunlight before entering our atmosphere is called the *total solar irradiance* (TSI) and is approximately 1361 W/m^2 at mean sun-earth distance (Cahalan, n.d.). This irradiance is the maximum amount of power that reaches the earths atmosphere, also known as the *air mass* (AM) 0 condition. AM refers to the pathlenght traveled by light relative to zenith pathlenght.
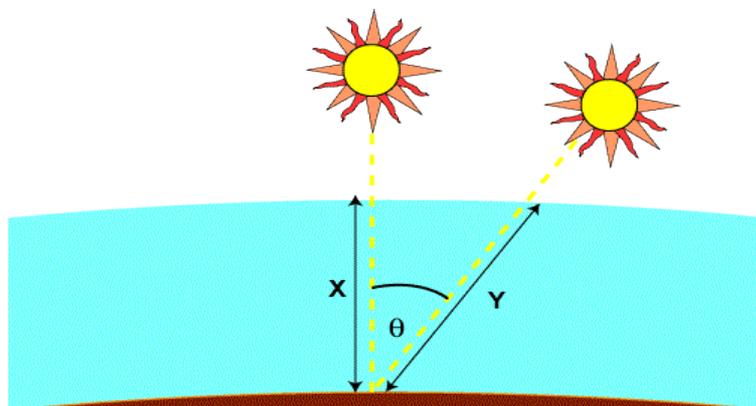
Illustration 6: Air mass concept, AM = Y/X, (Bowden and Honsberg, n.d.)

Available power decreases as light propagates through the atmosphere due to interactions with atoms and molecules. These interactions lead to scattering of incoming light and atmospheric heating (i.e. earthbound power decreases). Higher AM means longer pathlenght and hence lower power. Interaction with the atmosphere also changes the light spectra (e.g. ozone absorbing UV-light).

Light approaching a surface can be divided into *direct* and *diffuse* light. Direct light is photons coming from the disc of the sun. Diffuse light is photons that has been scattered in the atmosphere. The *global irradiance* at ground level is the sum of direct and diffuse light. *Insolation* is irradiance integrated over time, and thus represents the amount of energy received by a given area (i.e. kWh/m^2).

Standard testing conditions (STC) for solar cells in a laboratory environment are set to AM 1.5 spectral distribution and 1 kW/m^2 global irradiance (Luque and Hegedus, 2011). AM 1.5 is seen as an average spectrum for much of the developed world, approaching AM 2.0 in the northernmost parts of our globe. The spectrum and intensity changes as the position of the sun relative to a photovoltaic device changes (i.e. day-night cycle), affecting system performance.

Actual irradiance and annual insolation at ground level is what's important for photovoltaic devices. Data for mean irradiance and insolation exists for a large number of locations (e.g. the Atmospheric Science Data Center at NASA, (Stackhouse, 2012)).

6.2 Major photovoltaic cell types and efficiencies

Two main categories of photovoltaic cells exists to this date: crystalline silicon wafer cells and thin-film cells. Crystalline silicon cells consist of wafers made out of solar-grade or electronic-grade silicon. Electronic-grade silicon have higher purity than necessary for photovoltaic production but has been used historically due to low demand for solar-grade silicon. The wafers are etched in order to lessen surface reflections and increase the distance a photon needs to travel, thus increasing probability of absorption. The wafer material is doped with a p-type dopant during the manufacturing process. Wafer front-end is then doped with an n-type dopant through a diffusion process, which creates the necessary n-p junction. Contacts are printed on the front- and backside of the cell and coated for protection and enhanced optical performance. See *Appendix D* for a short overview of the photovoltaic effect. (Corkish, 2006)
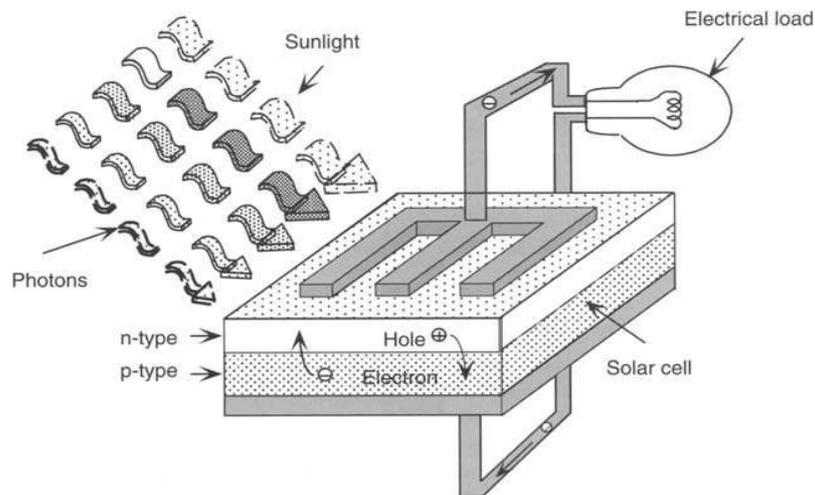
Figure 2: General cell structure (Corkish, 2006)

Aberle (2009) offers a short overview of the major thin-film technologies. Thin-film cells is made from deposition of semiconductor vapors onto substrates or superstrates. A transparent conducting oxide (TCO) generally forms the front contact, upon which doped semiconductor layers is deposited to form the p-n junction. Amorphous silicon, microcrystalline, CdTe and CI(G)S are examples of thin-film cells. Silicon approaches needs to be doped by addition of hydrogen and- or silicon carbide in order for a junction to form, whereby junctions form naturally for CdTe and CIS cells. Some cells may have reflective back-coating to utilize more sunlight, or just a simple metallic rear contact. Efficiencies do generally not reach the levels of wafer-based cells as of 2012. CIGS and CdTe thin-film cells carry the burden of relying on rare metals not readily available.

Table 6.1: Reported maximum efficiency values for major PV technologies under AM 1.5 conditions at cell level (Green et al., 2012) and average efficiencies (Frankl and Nowak, 2012)

	η_{max}	η
Monocrystalline	0.25	0.14-0.20
Polycrystalline	0.204	0.13-0.15
Amorphous Si cell	0.101	0.06-0.09
CdTe	0.167	0.09-0.11
CI(G)S	0.196	0.10-0.12

Polycrystalline ribbon cells show somewhat lower maximum efficiencies than conventional polycrystalline Derbouz et al. (2012) and Kim et al. (2006). Panel efficiency is generally lower than cell efficiency. A PV panel based on wafer cells will have inactive areas (i.e. spacing between cells) not able to convert incoming sunlight to energy. Yields are lowered even further due to optical losses in the panel front cover- and coating and resistive losses in cell-to-cell wiring. These losses cause the typical panel efficiency to be approximately 10-15% lower than cell efficiencies, although panel efficiency losses have been reduced to 5% under laboratory conditions (Fraunhofer ISE, 2011).

Table 6.2: Typical panel efficiencies as reported by Fthenakis and Kim (2011) and Jungbluth et al. (2012)

	η
Monocrystalline Si	0.14
Polycrystalline Si	0.132; 0.136
Ribbon Si	0.115; 0.125

Efficiency and power rating for a particular type of cell/panel are measured under standard reference conditions: AM 1.5 spectra, irradiance ($G_{g,STC}$) of 1000 W/m^2 and 25 degrees Celsius. Modeling the AM 1.5 spectra in a laboratory environment can be problematic and will give rise to errors regarding maximum efficiency. Power rating is reported as *kilowatt peak* (kW$_p$) and reflects the power output when standard reference conditions prevail, although these conditions are not very common in the real world. The actual power output depend on a large number of variables such as temperature, weather, orientation, sunlight spectra etc. which makes photovoltaic power output very site-dependent. (Luque and Hegedus, 2011)

PV cell/panel efficiency can be thought of as:

$$\eta = \frac{P_{DC}}{G_g \cdot A} \qquad (8)$$

where P_{DC} is cell/panel power output, G_g is global incident irradiance and A is cell/panel area. This approach is general and straightforward. STC conditions give an efficiency η_{STC} often used for efficiency rating. A more efficient cell/panel type will use comparatively less area to provide any given power rating. This conversion efficiency is rarely reached in the field since shading, temperature and soiling will affect efficiency.

6.3 Energy output

A simplified method for finding the energy produced by a photovoltaic unit is given below, based on known, general energy-delivering principles of incoming energy and conversion efficiencies. The theoretical maximum energy produced can be found by solving for P_{DC} in (12) and integrating over a time-period t, noting that irradiance varies over time and that integration over time yields *insolation* (H_g):

$$E_{DC}(t) = \int_0^t \eta \cdot A \cdot G_g(t) dt = \eta \cdot A \cdot H_g \qquad (9)$$

This assumes that efficiency is constant, which under real conditions is untrue. The delivered power/energy must then pass through BoS components (e.g. inverter), further reducing yield:

$$\eta_{BoS} = \frac{P_{AC}}{P_{DC}} \qquad (10)$$

Actual operational efficiency may not be known before deployment (e.g. at least not for back-of-envelope calculation purposes), but η_{STC} might be known. Dividing lifetime/annual/monthly/daily insolation H_g with $G_{g,STC}$ gives *amount of time* under an average irradiance of 1 kW/m^2 (i.e. standard testing conditions), at least with respect to incoming *solar power*. If the cell/panel/array rating is known one can also (approximately) calculate delivered energy according to:

$$E_{AC}(t) = \eta_{BoS} \cdot P_{DC,STC} \cdot \frac{H_g(t)}{G_{g,STC}} \qquad (11)$$

Internet databases containing solar irradiation data by geographic location is freely available, often containing interactive interfaces able to calculate potential photovoltaic energy production. These interfaces can take a lot of factors into consideration (e.g. ambient and operating temperature, time-varying irradiance and mounting angles), producing data output regarding expected energy delivery in a certain location. PVWATTS (NREL, 2012) and PV-GIS (JRC, 2012) are two examples of such software provided by the U.S National Renewable Energy Laboratory and EU Joint Research Commission respectively. These tools (primarily PV-GIS) will be used for all energy output calculation purposes in this thesis due to the high level of detail and ease of use. This tool also take relative efficiency losses due to ambient temperature fluctuations into consideration. Documentation for both PV-GIS and PVWATTS is available online.

7   Model description

Below follows a description of the processes and assumptions included in the process-chain model. The chain consists of the processes directly affiliated with silicon processing, but does not include the quartz mining. Embodied energy enters the system as aluminum, copper, steel, SiC, concrete and glass at different stages. See *Illustration 1* for visualization of the *reduced system*. *Appendix A* contains an example on how the CED for c-Si panels using extended system boundaries are calculated.

7.1   Metallurgical-grade silicon

Silicon is an abundant element in the earths crust and is almost exclusively found as silica in sand and quartz. The silica feedstock is mixed with a carbon source (charcoal, coal, coke or wood chips) in an electric arc furnace where a reduction reaction takes place. Electric heating and release of chemical energy from the reduction agent fuels this process. Reduction agent consumption is in a strict sense a non-energy input, but is treated as an energy input since (some of) the reduction agents have alternative use as energy carriers. The result is a high-purity silicon smelt with some impurities and exhaust gases.

Data and process description presented in Jungbluth et al. (2012) is used as source material. The consumed electric energy is assumed to consist of hydropower, as metallurgical industries often have separate contracts with hydropower utilities (Jungbluth et al., 2012). Energy content data for reduction agents were provided by IEA et al. (2005).

Table 7.1: Energy demand for production of mg-Si

	MJ_{PE} / kg_{mg-Si}	Comment
Electric energy	40	Hydropower
Heat	41	

7.2   Silicon carbide

Silicon carbide is used as an abrasive cutting medium in wafer wire-cutting. The slurry is sprayed onto the cutting wires and constitutes the "teeth" of the wire. Silicon carbide is produced by mixing silica and a carbon source under high-temperature conditions (i.e. carbothermic reduction). After cutting the used slurry is recycled and reintroduced into the slurry stream. The recycling process requires approximately 6% of the energy necessary to produce virgin SiC. (Jungbluth et al., 2012)

Table 7.2: Energy demand for production of SiC

	MJ_{PE} / kg_{SiC}	Comment
Electric energy, primary SiC	100	UCTE
Heat, primary SiC	39	
Electric energy, recycled SiC	9	UCTE

7.3   Solar-grade silicon

Metallurgical-grade silicon has a purity of 98-99% silicon, which is insufficient for photovoltaic applications. Jungbluth et al. (2012) states that further purification is needed for PV applications. The produced silicon must reach a purity of at least 6N (99.9999%). The purity level for electronic-grade silicon is even higher. Electronic-grade silicon consists of extremely pure silicon (e.g. 9N or 99.9999999%). Such high-purity silicon is achieved through the Siemens-process. This purity is in excess of what is needed for PV applications, but has been used historically in conjunction with off-grade silicon from the aforementioned process due to low demand for solar-grade silicon. As demand for solar-grade silicon has gone up, so has the need for a dedicated process-route. (Müller et al., 2006)

7.3.1 Modified Siemens-process

The Siemens-process is energy-intensive and essentially means that metallurgical-grade silicon is turned into silane (SiH_4) or trichlorosilane ($HSiCl_3$) which is fed into a reactor. These gases decompose at a certain temperature, resulting in the deposition of silicon. Filtvedt et al. (2010) offer a short overview of the process. A common name for this type of technique is *chemical vapor deposition* (CVD). A Siemens-reactor consists of u-shaped silicon core rods which is heated electrically. The silane or trichlorosilane reacts at the surface of these heated rods, depositing additional silicon. The reactor walls needs to be cooled in order to avoid unintentional and unwanted deposition. The rods are removed from the reactor once target size has been reached.
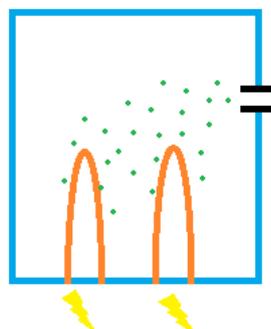

Illustration 7: Siemens-process reactor concept

A *modified Siemens-process* is examined in this thesis. The regular Siemens-process is modified to yield silicon of lower quality (i.e. SoG-Si). The modified process requires less energy than the conventional Siemens-process. (Jungbluth et al., 2012)

The energy-demand data in the table below is imported from Jungbluth et al. (2012). The production of one kilogram SoG-Si requires 1.13 kg of mg-Si.

Table 7.3: Energy demand for modified Siemens-process

	MJ_{PE} / kg_{SoG-Si}
Electric energy	590
Process heat	185

7.3.2 Fluidized bed and metallurgical route for SoG-Si

The chemical vapor deposition mechanism used in the Siemens-process can also be used in a fluidized bed reactor. Silicon seed particles are introduced into a reactor vessel, heated and fluidized. The FBR-CVD process is less energy-intensive compared to the Siemens-process, partly because of the decreasing importance of internal wall cooling. See Filtvedt et al. (2010) for a short description.

Jungbluth et al. (2012) provides information regarding energy demand for FBR-CVD, although no complete LCI has be found.

Table 7.4: Energy demand for SoG-SI through FBR

	MJ_{PE} / kg_{SoG-Si}
Electric energy	500

The metallurgical route produces what is known as *upgraded metallurgical silicon*. One example of such technique is the proposed Elkem-process. Conventional mg-Si production is combined with slag treatment, chemical leaching and directional solidification (Glockner et al., 2008).

Data from Glockner et al. (2008) has been used to examine the impact of introducing the Elkem metallurgical route instead of the Siemens-process.

Table 7.5: Energy demand for SoG-Si production through metallurgical route

	MJ_{PE} / kg_{SoG-Si}
Electric energy	140
Embodied energy	180

7.4 Czochralski process

The use of monocrystalline silicon gives the highest quality solar cells. A monocrystalline is ideally a single, unbroken crystal. Monocrystalline (c-Si) silicon ingots are commonly produced through the Czochralski process. Solar- or electronic-grade silicon are melted in a crucible. A seed crystal is introduced into the melt and allowed to grow. The crystal is then continuously pulled out of the melt and cooled as the desired diameter is reached.
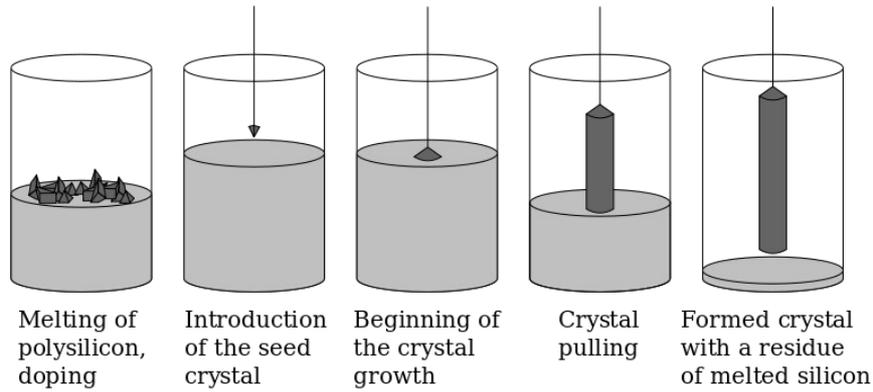
Illustration 8: Czochralski process

This process is according to Jungbluth et al. (2012) very energy-intensive. 1.07 kg SoG-Si is required in order to produce 1 kg c-Si. Electric energy is used for heating as well as cooling.

Table 7.6: Energy demand Czochralski process

	$MJ_{PE} / kg_{c\text{-}Si}$	Comment
Electric energy	996	UCTE
Heat	62	Natural gas

7.5 Multicrystalline silicon ingot casting

Silicon ingots which consists of multiple crystals are said to be multicrystalline (mc-Si). These crystals have poorer electrical properties than monocrystalline silicon. Schönecker et al. (2003) offer a summary of the casting processes. Multicrystalline ingots are produced by melting solar-grade silicon in a crucible and simply letting the melt cool and solidify. The solidification process is performed either through conventional multi-crucible casting methods or by moving the crucible in relation to heating equipment, allowing for directional solidification. A multicrystalline silicon ingot ideally consists of columnar grains of monocrystals. The boundaries between these grains negatively affects electrical properties (Corkish, 2006). The data-set offered by Jungbluth et al. (2012) show an energy demand for mc-Si that is considerably lower than for c-Si. One kilogram of mc-Si requires 1.18 kg of SoG-Si.

Illustration 9: Mutlicrystalline casting technologies

Table 7.7: Energy demand for multicrystalline silicon casting

	MJ$_{PE}$ / kg$_{mc-Si}$	Comment
Electric energy	224	UCTE

7.6 Wafer sawing

The ingots produced by the Czochralski-process (c-Si) and silicon casting (mc-Si) needs to be cut into thin wafers. The cylindrical ingots from the Czochralski-process are cropped to p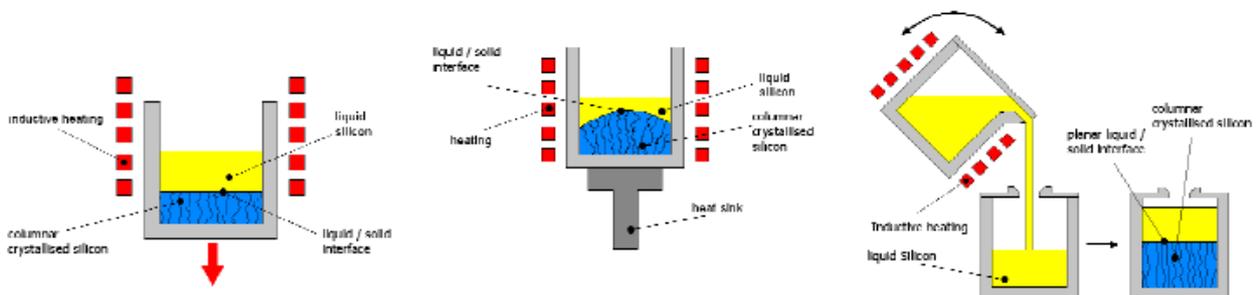roduce ingots with rectangular sides, and the multicrystalline ingots are cut at the ends to remove impurities (Xakalashe and Tangstad, 2011). Ingots are then placed under a mesh of parallel tightened wires onto which an abrasive slurry of silicon-carbide (SiC) sticks. The wires are moved back and forth and the sawing slurry act as a cutting medium, producing wafers with a thickness of approximately 200 μm. The area under these sawing wires is lost as sawdust (i.e. kerf loss) and causes approximately 50% of the ingot material to be lost (Jungbluth et al., 2012).

Jungbluth et al. (2012) states that one m^2 of c-Si and mc-Si wafer weighs 0.443 and 0.466 kg respectively. Assuming a 50% kerf loss means the silicon demand for a wafer area of one square meter is 0.885 kg/m$^2_{c-Si}$ and 0.932 kg/m$^2_{mc-Si}$. The sawing of one square meter requires 0.49 kg primary SiC and 2.16 kg recycled SiC.

Wafers can also be produced through processes where ribbons of molten silicon are directly cast and solidified into wafers. This eliminates the kerf-loss, although wafers still need to be sawed into the desired shape. The cut-offs can be melted and reintroduced into production. Ribbon-based silicon wafers are somewhat thicker than c-Si- or mc-Si wafers, reaching a weight of 0.583 kg/m$^2_{r-Si}$. Including some losses (e.g. breakage and cut-off loss) means that production of one square meter of r-Si has a silicon demand of 0.739 kg/m$^2_{r-Si}$ (Jungbluth et al., 2012).

Table 7.8: Energy demand for producing c-Si, mc-Si and r-Si silicon wafers

	MJ$_{PE}$ / m^2	Comment
Electric energy	92.9	UCTE
Heat	4	
Wafer, r-Si	490	Smelting & casting

It's important to realize that the energy demand for ribbon-based wafers include *both* smelting and casting. This technique further uses less material per square meter due to the absence of kerf loss. The result is a lower *CED* per square meter when compared to wafers originating from sawed ingots.

7.6.1 Kerf loss

Jungbluth et al. (2012) states that approximately half the silicon ingots are lost due to kerf losses. The sawing dust is mixed with the abrasive sawing slurry. The used sawing slurry can be recycled, but there is currently no commercially available process able to recycle the sawing dust. There is however ongoing work withing this field. Wang et al. (2009) present a method for doing so, the resulting silicon being pure enough to produce cells with efficiencies of 12.6%. The study compared this efficiency with that from a commercially available cell which had an efficiency of 14%. One of the main challenges seem to be the separation of crushed SiC-particles, metal from the sawing wire and the silicon dust as these are not easily separated. The report concludes that almost all SiC was removed from the recycled silicon. No energy-demand data for this process has been found.

7.7 Cell production

A wafer needs to be turned into a *cell* before any energy-production can occur. Jungbluth et al. (2012) and Corkish (2006) offers an overview of this process. The wafers are etched by acid to remove surface damage due to sawing. Wafers also need to be doped with an n-type dopant (e.g. phosphorous) in order for the p-n junction to form. The dopant diffuses into the wafer material during heating. The outermost layer is heavily doped to improve electrical properties. A metallization paste is then printed on the wafer. This paste is burned into the wafer surface inside a furnace, forming the cell contacts. An anti-reflective coating is then applied to the cell surface.

Producing a photovoltaic cell requires many chemicals for etching, doping, cleaning and contact printing. The energy demand for producing these chemicals have not been included in the reduced system. One square meter of photovoltaic cell uses 1.06 m^2 of wafer for each cell type due to shape sawing (Jungbluth et al., 2012).

Table 7.9: Energy demand for cell production

	MJ$_{PE}$ / m^2	Comment
Electric energy	351	UCTE
Heat	6	

7.8 Aluminum production

Jungbluth et al. (2012) provides no information regarding the energy embodied in aluminum, so another data source has been used. The aluminum for panel framing constitutes a substantial amount of energy demand for the assembly process. European Aluminum Association (EAA) have published a LCA/LCI for aluminum production in Europe. The cumulative energy demand presented in this report can be seen as representative of actual energy demand.

The data covers everything from bauxite mining to profile extrusion, with the smelting stage absolutely dominating the energy demand. Usage of recycled material at the casting stage is included, which lowers total energy consumption. This refers to aluminum recycled in-house (i.e. primary aluminum saw-offs and waste re-smelted). Recycling of external aluminum (e.g. aluminum cans) is not included. (EAA, 2008)

Table 7.10: Energy demand for aluminum production

	MJ$_{PE}$ / kg	Comment
Electric energy	137	EAA thermal efficiency
Heat	52	

7.9 Glass production

Glass contributes a very large mass fraction per square meter of solar panel. PE International have, on behalf of the Glass for Europe association, performed a LCA regarding primary glass production (Usbeck Carrillo et al., 2010). The UCTE grid thermal efficiency is assumed for European glass production. Only 0,26 MJ$_{PE}$/kg of the energy demand is covered by renewable energy, the rest comes from non-renewable sources.

Table 7.11: Energy demand for glass production

	MJ$_{PE}$ / kg	Comment
Electric energy	2.6	UCTE
Heat	9	

7.10 Panel- and laminate assembly

A panel consists of several interconnected cells in series, resulting in a raised voltage compared to the voltage across the individual p-n junctions. The cells are embedded between thin sheets of ethylvinylacetate. A non-transparent film is placed in the back, and a glass panel with high transparency is placed over the front. This assembly is joined together under heat and pressure. A supporting frame of aluminum is attached around the cell assembly, completing the *panel*. One could also chose not to attach the aluminum frame, producing a *laminate*.

Energy expenditure and material requirements for panel assembly are found in Jungbluth et al. (2012). One m^2 of panel/laminate consists of 0.932 m^2 of cells due to spacings between the individual cells. The aluminum frame and glass cover weighs 2.63 kg/m^2 and 10.1 kg/m^2 respectively. These two inputs have the largest individual mass during the assembly process. Especially the production of aluminum is known to be energy-intensive. Other material inputs for this process are not included in the reduced system core. Energy demand for producing one m^2 of panel, including energy embodied in aluminum and glass thus becomes:

Table 7.12: Energy demand for assemblies, including indirect embodied energy

	MJ$_{PE}$ / m^2	Comment
Electric energy	55	UCTE
Heat	5	
Aluminum, embodied energy	496	
Glass, embodied energy	119	

This is comparable to the energy necessary for the Siemens-process. The high amount of energy needed can be attributed to the energy-intensive process of producing aluminum, which embodies a large amount of energy.

7.11 Copper production

Copper is used for transformers and in copper wiring used for the BoS components. Norgate et al. (2007) have performed an LCA of the environmental impacts for different metal production processes, of which copper is one. Energy demand is reported as primary energy demand.

Table 7.13: Energy demand for copper production

	MJ$_{PE}$ / kg
Smelting + electro-refinement	33

7.12 Stainless steel production

Stainless steel is used for panel mounts and for inverter casing primarily (in this data set). This is

included in the analysis as it is considered a bulk material that is known to be energy-intensive. Johnson et al. (2008) states that primary energy demand per kg of stainless steel is:

Table 7.14: Energy demand for steel production

	MJ_{PE} / kg	Comment
Energy	53	50% recycled steel

The analysis is a process-chain analysis including transports, and the main energy expenditure occurs during the smelting and alloy production stages.

7.13 Concrete production

A free-standing (i.e. not building mounted) photovoltaic plant uses concrete for a number of applications. Frames and fence poles are mounted in piled holes which may need to be filled with concrete for stability. Large concrete foundations are needed if heavy tracking devices are used or if ground conditions are unfavorable. Prieto and Hall (2013) state that the embodied energy in concrete (assumed to be non-reinforced) is 1 MJ_{PE} per kg.

7.14 Balance of system components

The panel is itself not enough when it comes to delivering actual useful power to society. Multiple panels needs to be connected in an array to deliver any meaningful amount of power to a building or grid, and delivered electric energy needs to be transformed from DC to AC. Mounting structures, cabling, metering equipment and inverters are thus necessary for power delivery. The reduced system in this thesis only include the inverter and mounting systems, not cabling or other auxiliary equipment.

Jungbluth et al. (2012) presents energy and material demand data for inverter manufacture and material necessary (i.e. aluminum and steel) for different mounting options. An inverter consists of power electronics and transformers in a case. Inverter weight per nominal kW generally decrease as the nominal power rating increases, which means that energy demand induced by inverter production becomes less and less important as plant size increases. Direct energy expenditure for inverter production and energy embodied in the aluminum, copper and steel are assumed to be the most relevant inputs. The inverter size deemed most relevant for use in medium-sized system mounted or integrated on buildings is an inverter with a nominal rating of 2.5 kW. This would require 1.4 kg of aluminum, 5.51 kg of copper and 9.8 kg of steel for casing and wiring (note: this is an absurd amount of steel and copper for a modern inverter. Data is however kept in order to harmonize with other ecoinvent-data used). All inputs are downscaled to correspond to an inverter capacity of 1 kW. The BoS efficiency η_{BoS}, including inverter and cabling losses as well as occasional soiling, is set at 0.86. This is the default value recommended by the PV-GIS tool (JRC, 2012).

Table 7.15: Energy demand for inverter production, including indirect embodied energy

	MJ_{PE} / kW	Comment
Aluminum, embodied energy	106	
Copper, embodied energy	73	
Steel, embodied energy	208	
Electric energy	98	UCTE

Two principal options exists when mounting a photovoltaic panel on buildings: building-integration or frame-mounting (Jungbluth et al., 2012). A panel for frame-mounting means that the laminate needs an aluminum profile to enable frame mounting. This profile is accounted for in the panel-production stage. The actual frame requires an additional 2.8 kg/m² and 2.5 kg/m² of aluminum for slanted- and flat-roof mounting respectively. Steel requirements amount to 1.5 kg/m² for slanted roofs and 0.3 kg/m² for flat roofs. Energy required for mounting labor is considered insignificant compared to other requirements.

PV panels without aluminum profiles are called laminates. These laminates can be integrated into buildings (e.g. exterior walls, slanted roofs) by providing a framework of aluminum- and steel mounting structures. The weight of these structures amount to 2.2 kg/m² of aluminum and 0.2 kg/m² of steel.

Table 7.16: Embodied energy demand for slanted roof frames, indirect embodied energy

	MJ_{PE} / m² (panel size)
Aluminum, slanted roof	528
Steel, slanted roof	80

Table 7.17: Embodied energy demand for slanted roof profiles, indirect embodied energy

	MJ_{PE} / m² (laminate size)
Aluminum, slanted roof, integrated	415

Table 7.18: Embodied energy demand for facade frames, indirect embodied energy

	MJ_{PE} / m² (panel size)
Aluminum, facade	490
Steel, facade	95

Illustration 10: BoS components. Cabling, inverter (with case) and mounting frame.

7.15 Area, energy demand and kW$_p$

The kilowatt-peak (kW$_p$) is chosen as the functional unit as this allows for easy comparison between the energy demand of different PV technologies. An efficient panel will require less area than a less efficient one in order to produce one kW$_p$ during STC. Less area requirement results in a lower cumulative energy demand. The area required to produce one kW$_p$ can be found via:

$$A_{kW_p} = \frac{G_{STC}}{\eta_{STC}} \qquad (12)$$

where G$_{STC}$ is the irradiation and η_{STC} is the efficiency under STC (G$_{STC}$ = 1000 W/m^2). This area requirement is then multiplied by the cumulative energy demand for one m^2 of panel and the energy demand for inverter added. The result is the total cumulative energy demand for the system at hand.

7.16 Performance degradation

The energy production capabilities decrease over a PV system's lifetime. Arrays installed in the 1990s are just now reaching 20 years in operation, and the current lifetime of systems is projected to be around 25-30 years. Continuous exposure to sunlight may affect the EVA-foil negatively and electrical components deteriorate over time. Mechanical damage is not uncommon, the outdoors being a rather harsh environment. Discoloration of the panels are common. A study by Polverini et al. (2012) concludes that the power production of an array in Italy consisting of mc-Si modules decayed by 0.24% per year over a period of 19 years. Jordan and Kurtz (2013) cite a median degradation rate of 0.5% per year and a mean rate of 0.8%, derived from a very large amount of studies. This is the median for both thin-film and crystalline silicon modules and systems examined. Approximately 78% of all measured decay rates where found to be below 1% per year. An annual degradation rate of 0.5% over the 30 year lifetime is used in this thesis.

7.17 Extended system boundaries

This thesis utilizes a simple, reduced system sprung out of the data available in Jungbluth et al. (2012) combined with *external* (i.e. non-ecoinvent) data sources for processes which are known to be energy-intensive. The completeness of the system in this thesis compared to the original system by (Jungbluth et al.,2012) could possibly be assessed by comparing CED's. Jungbluth et al. (2012) presents a CED for the c-Si and mc-Si which has been calculated by LCA software (likely SimaPro) using the ecoinvent database. CED is given per produced kWh, but the annual production per kW$_p$ (922 kWh/kW$_p$) and system lifetime (30 years) is known. The CED per kW$_p$ can be calculated/back-traced from this information.

Table 7.19: Cumulative energy demand per kW$_p$, extended system

	c-Si	mc-Si
Jungbluth CED [MJ$_{PE}$]	40107	35958

Table 7.20: *Cumulative energy demand per kW$_p$. reduced system*

	C-Si	mc-Si
This thesis CED [MJ$_{PE}$]	26010	22142

Ecoinvent data-sets contain pointers to other technosphere objects and processes, which is easily added to the system modeled in LCA software (e.g. SimaPro) (Frischknecht et al., 2007). The linking of data-sets and possible "automatic crawling" through sub-sets by LCA software not possible in the manual approach could explain the significant gap in energy demand. If the LCIA has been performed in such a mode then it's likely that the Jungbluth et al. CED also has included energy expenditure for aluminum, steel, copper and glass plus a plethora of other materials and processes. This means embodied indirect energy is accounted for to a rather large extent (not just the explicit energy inputs following the silicon trail).
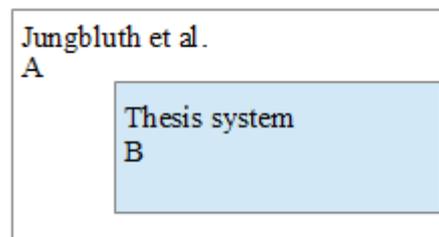
Illustration 11: Relationship between extended and reduced system boundaries

Subtraction of B from A approximately represent the processes not included in this thesis (e.g. transport, production of hydrochloric acid, EVA foil etc.). (A-B) can be treated as a "black box" and added to the modeled reduced system. It should be noted that, even though the difference in energy demand between these two systems are rather large, the *amount* of processes and material types are very different. The system in this thesis consists of approximately 40 inputs, to be compared with the data-tables in Jungbluth et al. (2012) which lists 200+ inputs. Around 40 out of *at least* 200 inputs cause approximately 60% of the CED. Electric energy use in just a few process steps (e.g. SoG-Si production, Czochralski ingot production and aluminum production) dominates the energy demand among these ~40 inputs.

Table 7.21: Energy demand difference between reduced system and Jungbluth et al. (2012)

	c-Si	mc-Si
A − B [MJ$_{PE}$]	14097	13816

EROI using the Jungbluth et al. system boundaries for c-Si and mc-Si panels becomes:

Table 7.22: *Default EROI using extended system boundaries*

	c-Si	mc-Si
$EROI_e$	4.09	4.57
$EROI_{PE}$	13.2	14.73

The EROI of c-Si and mc-Si panels become increasingly similar when adding the "rest" of the Jungbluth system. This could be explained by the fact that an increasing number of processes and inputs are now common and shared between these two panel types (i.e. the relative contribution of very energy-intensive steps like Czochralski ingot production is now less).

Ribbon-based multicrystalline panels are not assessed specifically in Jungbluth et al. but share many characteristics with mc-Si panels with the exception of one-step wafer production from silicon smelt and lower efficiencies.

8   Result

The reduced dataset compiled from Jungbluth et al. (2012) yield a cumulative energy demand for three types of silicon wafer-based solar panels. All three panel-types are assumed to be roof-mounted on a frame and having an inverter matching installed rated power (i.e. 1 kW_p). Energy output is found by using online estimation tools (JRC, 2012) and (NREL, 2012) regarding annual delivered PV electric energy and multiplying by system lifetime. Optimal insolation conditions for a fixed position are used, which generally means a tilt angle equal to geographic latitude and south- or north-facing azimuth angle depending on hemisphere location. Alsema et al. (2009) provides LCA guidelines for photovoltaics and suggests that an insolation of 1700 kWh/y is used. This corresponds to conditions in southern Europe around the Mediterranean sea (Sicily). Delivered electric energy is assumed to replace electric energy from the UCTE grid.

Table 8.1: Default EROI results using reduced system boundaries

	Efficiency	Panel area	Input [MJ_{PE}/kW_p]	Output [MJ/yr]	$EROI_{PE}$	$EROI_e$
c-Si, 1kW_p	0.14	7.14	26010	152796	18.95	5.87
mc-Si, 1 kW_p	0.136	7.35	22142	152796	20.26	6.28
r-Si, 1 kW_p	0,125	8	22569	152796	21.84	6.77

The EROI above are based on efficiencies used for impact assessment in Jungbluth et al. (2012), as this is the main source for LCI data used in this thesis. The impact of changing inputs and outputs for EROI are linear (numerator) or near-linear (denominator) (univariate analysis), so a sensitivity coefficient $\Delta_{EROI}/\%$ is given to indicate average sensitivity for each examined parameter.

8.1   Geographic dependence

The number one factor in energy produced by a PV system is the amount of sunlight received. This amount changes as the location change. A PV panel in the Saharan desert produce a lot more energy than the same panel placed in northern Sweden. Received insolation (and consequently delivered

electric energy) is changed between ±60% to model extremes like polar and Saharan conditions.

Table 8.2: Geographic dependence/insolation

	c-Si	mc-Si	r-Si	System boundaries
$\Delta EROI_{PE}$/%	0.19	0.223	0.218	B
$\Delta EROI_{e}$/%	0.06	0.069	0.068	B
$\Delta EROI_{PE}$/%	0.123	0.137	0.136	A
$\Delta EROI_{e}$/%	0.038	0.042	0.042	A

8.2 Efficiency

Solar cell efficiency does not directly affect produced energy when using one kW_p as the functional unit, it's rather the area requirement (and hence the energy demand) that is affected. The default efficiencies used is quite low compared to state-of-the-art efficiencies.

Table 8.3: Efficiency impact on EROI

	c-Si	mc-Si	r-Si	System boundaries
$\Delta EROI_{PE}$/%	0.183	0.213	0.209	B
$\Delta EROI_{e}$/%	0.057	0.066	0.065	B
$\Delta EROI_{PE}$/%	0.103	0.114	0.109	A
$\Delta EROI_{e}$/%	0.031	0.035	0.034	A

8.3 Aluminum

Aluminum production is very energy-intensive and also constitute a relatively large mass fraction of a PV system. The energy input data refers to primary aluminum production, including profile extrusion.

Table 8.4: Aluminum energy demand impact

	c-Si	mc-Si	r-Si	System boundaries
$\Delta EROI_{PE}$/%	0.052	0.075	0.079	B
$\Delta EROI_{e}$/%	0.016	0.023	0.024	B
$\Delta EROI_{PE}$/%	0.02	0.026	0.026	A
$\Delta EROI_{e}$/%	0.006	0.008	0.008	A

Another way of quantifying the impact of aluminum production is to investigate EROI sensitivity to amount of aluminum in the frames:

Table 8.5: Aluminum mass sensitivity

	c-Si	mc-Si	r-Si	System boundaries
$\Delta EROI_{PE}$/%	0.026	0.037	0.04	B
$\Delta EROI_e$/%	0.008	0.011	0.012	B

8.4 Wafer thickness

The mass of one square meter of wafer is dependent upon wafer thickness. The thinning (or thickening) of wafers means a change in embodied energy. Change in thickness of one m^2 is translated into a change in mass by using the density for silicon (ρ_{Si} = 2329 kg/m^3). Default thickness is 190 μm for c-Si, 200 μm for mc-Si and 250 μm for r-Si. Wafer thickness is varied between -60% to +60% compared to original thickness.

Table 8.6: Wafer thickness sensitivity

	c-Si	mc-Si	r-Si	System boundaries
$\Delta EROI_{PE}$/%	0.095	0.085	0.05	B
$\Delta EROI_e$/%	0.029	0.026	0.016	B
$\Delta EROI_{PE}$/%	0.034	0.027	0.015	A
$\Delta EROI_e$/%	0.010	0.008	0.005	A

8.5 Kerf loss elimination and recycling

The saws used for silicon ingot cutting induce kerf losses. Kerf loss refers to the silicon under the sawing wire. The kerf loss is mixed with the silicon carbide sawing slurry and exits the sawing process as waste. Elimination of kerf loss can be modeled in the thesis model at no energy expense. This is unrealistic under real conditions, but energy data for recycling has not been found since the technology has not been commercialized as of 2009 (Wang et al., 2009).

Table 8.7: Kerf loss recycling

	c-Si	mc-Si	r-Si	System boundaries
$\Delta EROI_{PE}$/%	0.07	0.061	-	B
$\Delta EROI_e$/%	0.022	0.019	-	B
$\Delta EROI_{PE}$/%	0.019	0.015	-	A
$\Delta EROI_e$/%	0.006	0.005	-	A

The thinning of wafers means that the relative kerf losses increase since the sawing-width is not assumed to decrease.

8.6 Solar grade silicon

The modified Siemens-process which results in the SoG-Si is one of the more energy-intensive processes within the process-chain. A variance in process efficiency is modeled by changing the energy demand from -60 % to 60 %.

8.6.1 Modified Siemens-process

Table 8.8: Energy demand for modified Siemens-process

	c-Si	mc-Si	r-Si	System boundaries
$\Delta EROI_{PE}/\%$	0.038	0.061	0.044	B
$\Delta EROI_e/\%$	0.012	0.019	0.014	B
$\Delta EROI_{PE}/\%$	0.014	0.020	0.014	A
$\Delta EROI_e/\%$	0.004	0.006	0.004	A

8.7 Silicon ingot- and ribbon production

Solar-grade silicon is melted into either mono- or polycrystalline silicon ingots through the Czochralski process or through regular casting. The Czorchralski-process is especially energy-intensive. Ribbon-based silicon wafers also consists of polycrystalline silicon, but no ingot is produced. Wafers are instead produced directly, whereas comparison with the two other melting and cooling processes should be done with care. The energy necessary to produce one kilogram of ingot for c-Si and mc-Si is varied ±60%, whereas the unit for r-Si is energy per m². Comparison of sensitivity between these categories should thus be done carefully.

Table 8.9: Energy demand ingot and ribbon production

	c-Si	mc-Si	r-Si	System boundaries
$\Delta EROI_{PE}/\%$	0.049	0.015	0.038	B
$\Delta EROI_e/\%$	0.015	0.005	0.012	B

8.8 UCTE grid

Some process-steps within the production chain draws heavily on renewable energy, primarily hydropower. This energy is, for the purposes of this thesis, converted directly into primary energy (i.e. 1:1). The renewable energy used can be exchanged for UCTE generation mix in order to model a process-chain relying heavily on fossil fuels for all panel manufacturing purposes.

Table 8.10: UCTE generation mix for all inputs, reduced system

	c-Si	mc-Si	r-Si
$EROI_e$	4.43	4.86	4.95
$EROI_{PE}$	14.3	15.69	15.96

8.8.1 Silicon carbide recycling

Much of the silicon carbide used in the sawing process is already recycled (i.e. 80%). By reducing the fraction of recycled slurry one can get an indication of the sensitivity. Ribbon-based photovoltaic cells is not sawed and thus requires no silicon carbide.

Table 8.11: Recycled fraction of SiC sensitivity

	c-Si	mc-Si	r-Si	System boundaries
$\Delta EROI_{PE}/\%$	0.014	0.02	-	B
$\Delta EROI_e/\%$	0.004	0.006	-	B
$\Delta EROI_{PE}/\%$	0.005	0.006	-	A
$\Delta EROI_e/\%$	0.002	0.002	-	A

8.9 Steel production

Steel is used in the support structures and inverter casing. Steel production could as such be an important factor regarding EROI for photovoltaics. The energy demand of one kilogram steel are changed by ±60%. Translating this into actual action could for example mean more or less recycled steel in mixture (directly affects energy demand). The amount of recycled scrap in the production mix is by default approximately 50%.

Table 8.12: Steel production energy demand sensitivity

	c-Si	mc-Si	r-Si	System boundaries
$\Delta EROI_{PE}/\%$	0.007	0.01	0.01	B
$\Delta EROI_e/\%$	0.002	0.003	0.003	B

8.10 Variable relationship

The obtained results are combined in a *spider-type* plot showing variable importance in relation to each other. This is mainly an indicator of sensitivity. The slope indicates EROI sensitivity for a certain variable. Mono-, multi- and ribbon wafers are displayed in individual plots. The overall pattern regarding variable importance is consistent; efficiency and insolation affects EROI more than any other factor.
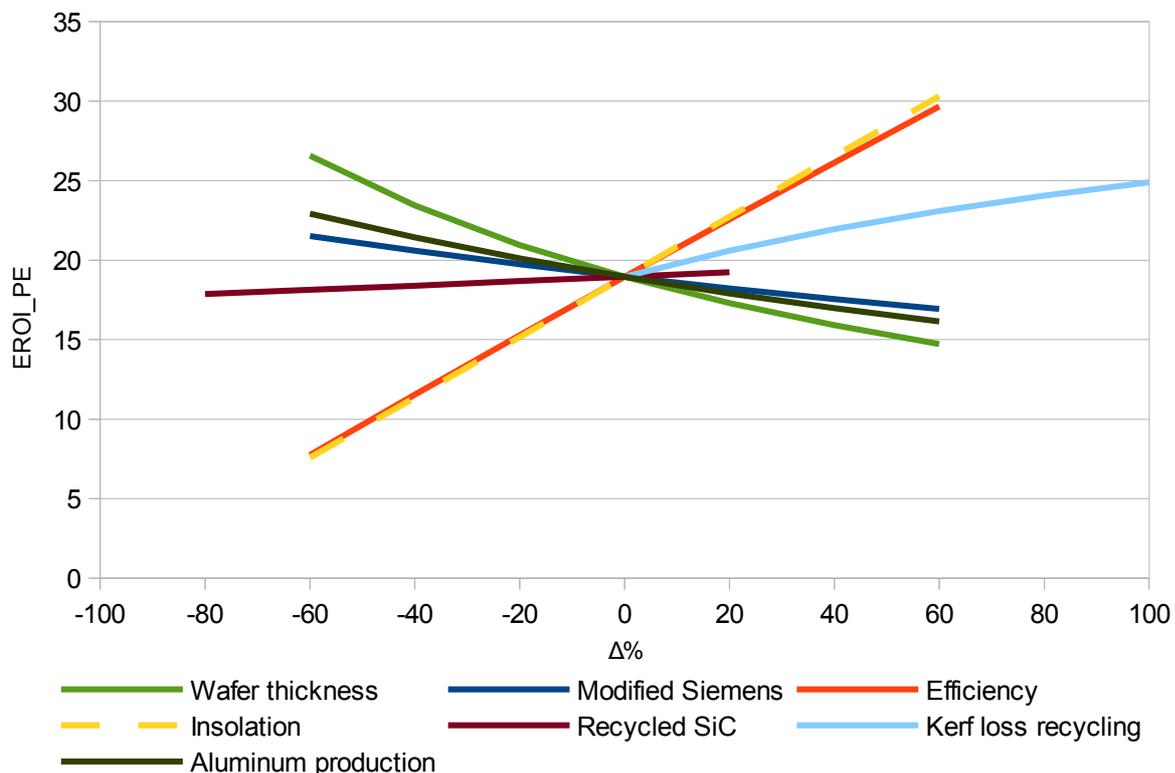

Illustration 12: Spiderplot c-Si, reduced system. "Modified Siemens" refers to energy requirement of the Siemens-process. "Aluminum production refers to energy requirement of aluminum production.

29

Illustration 13: Spiderplot mc-Si, reduced system. "Modified Siemens" refers to energy requirement of the Siemens-process. "Aluminum production refers to energy requirement of aluminum production.
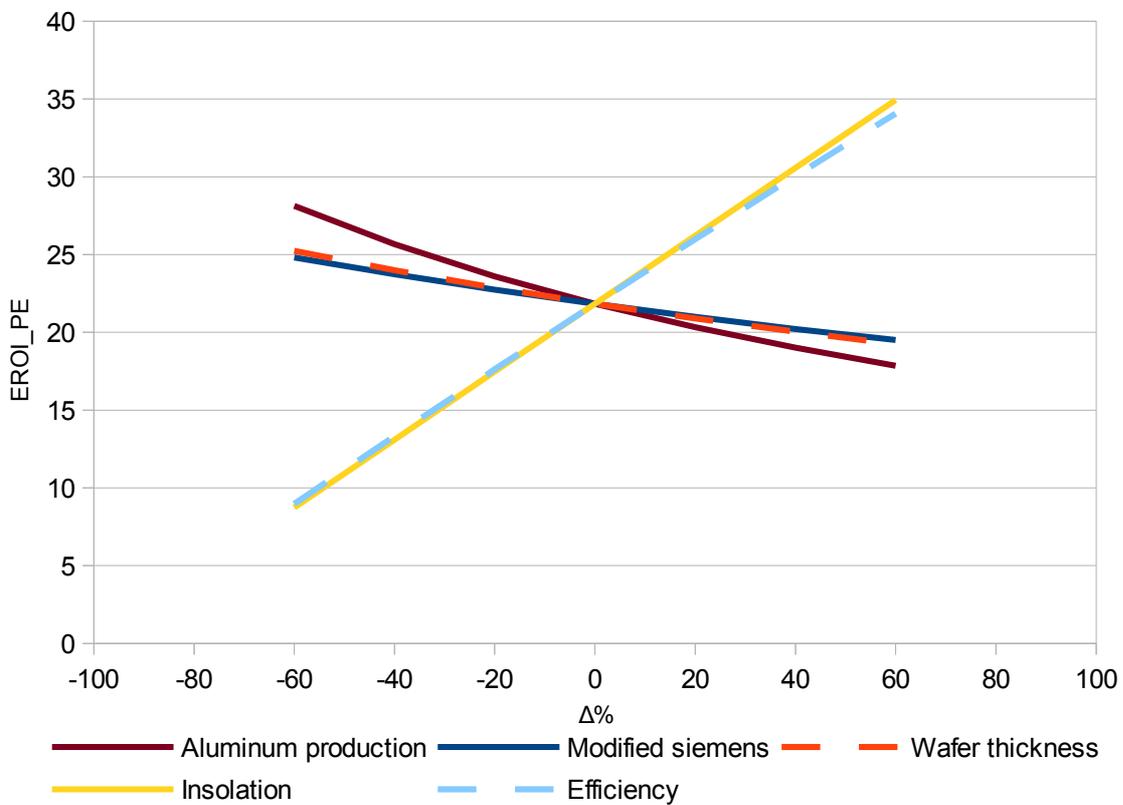
Illustration 14: Spiderplot r-Si, reduced system. "Modified Siemens" refers to energy requirement of the Siemens-process. "Aluminum production refers to energy requirement of aluminum production.

Illustration 15: Spiderplot c-Si, extended system. "Modified Siemens" refers to energy requirement of the Siemens-process. "Aluminum production refers to energy requirement of aluminum production.
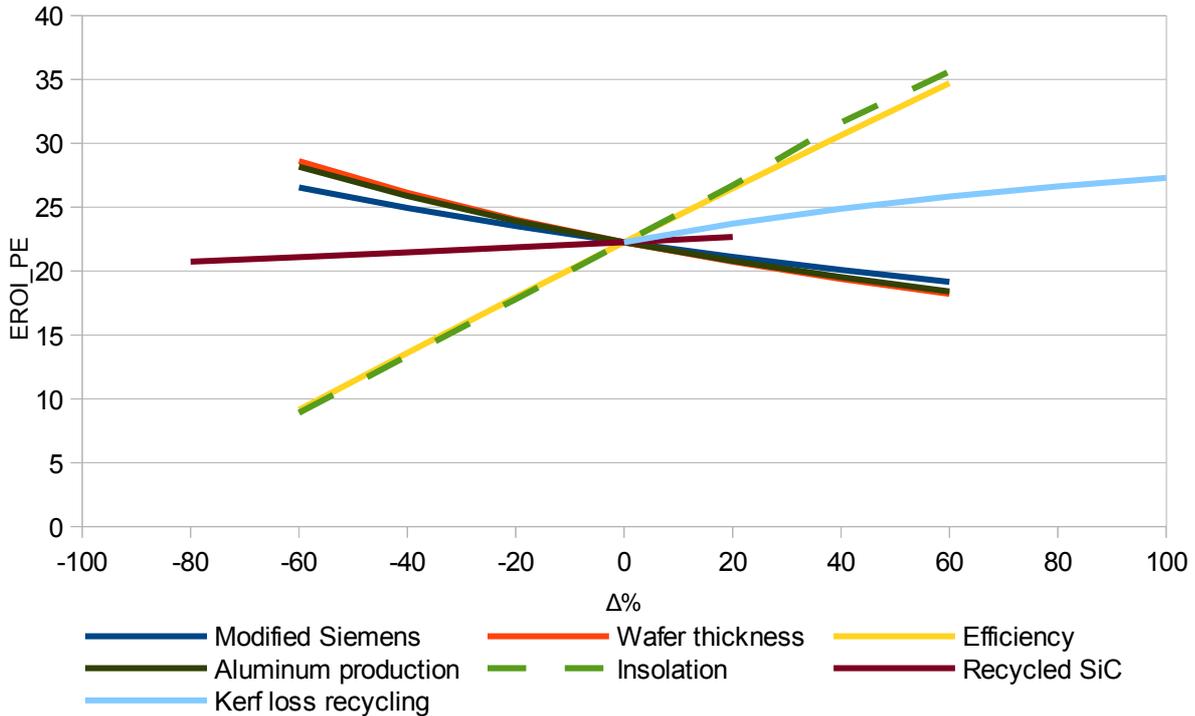

Illustration 16: Spiderplot mc-Si, extended system. "Modified Siemens" refers to energy requirement of the Siemens-process. "Aluminum production refers to energy requirement of aluminum production.

Illustration 17: Spiderplot r-Si, extended system. "Modified Siemens" refers to energy requirement of the Siemens-process. "Aluminum production refers to energy requirement of aluminum production.
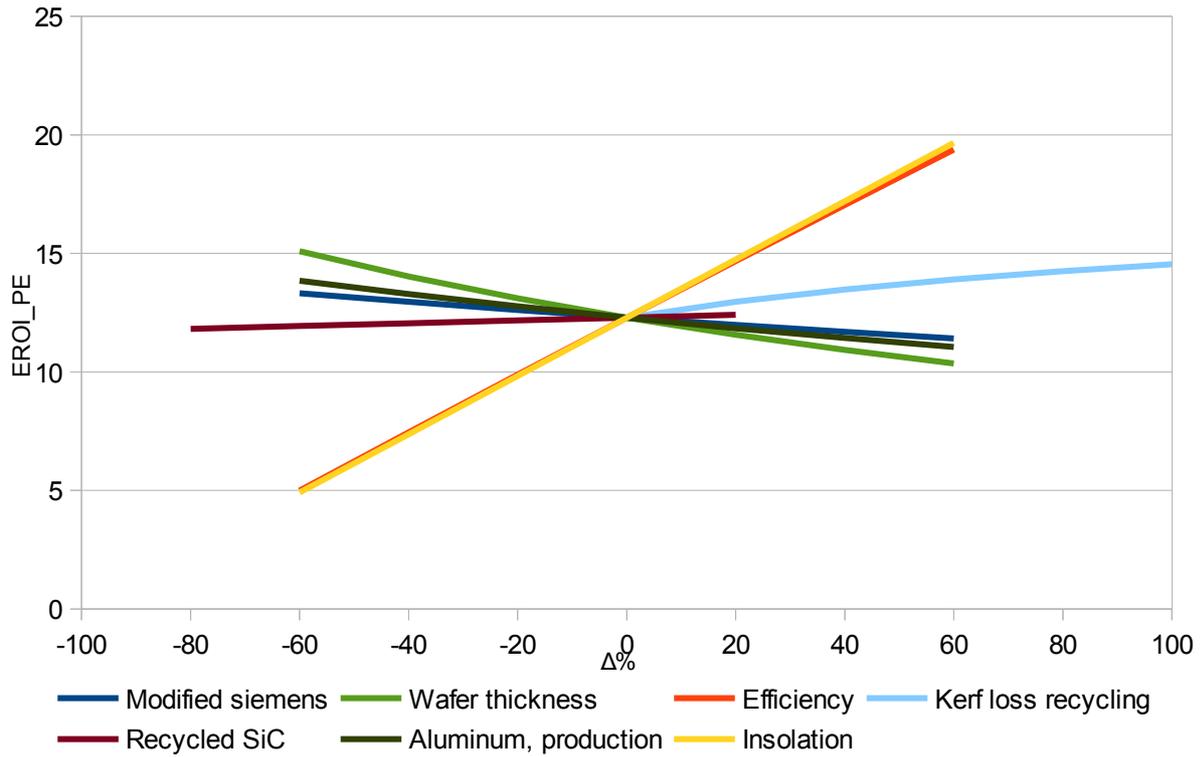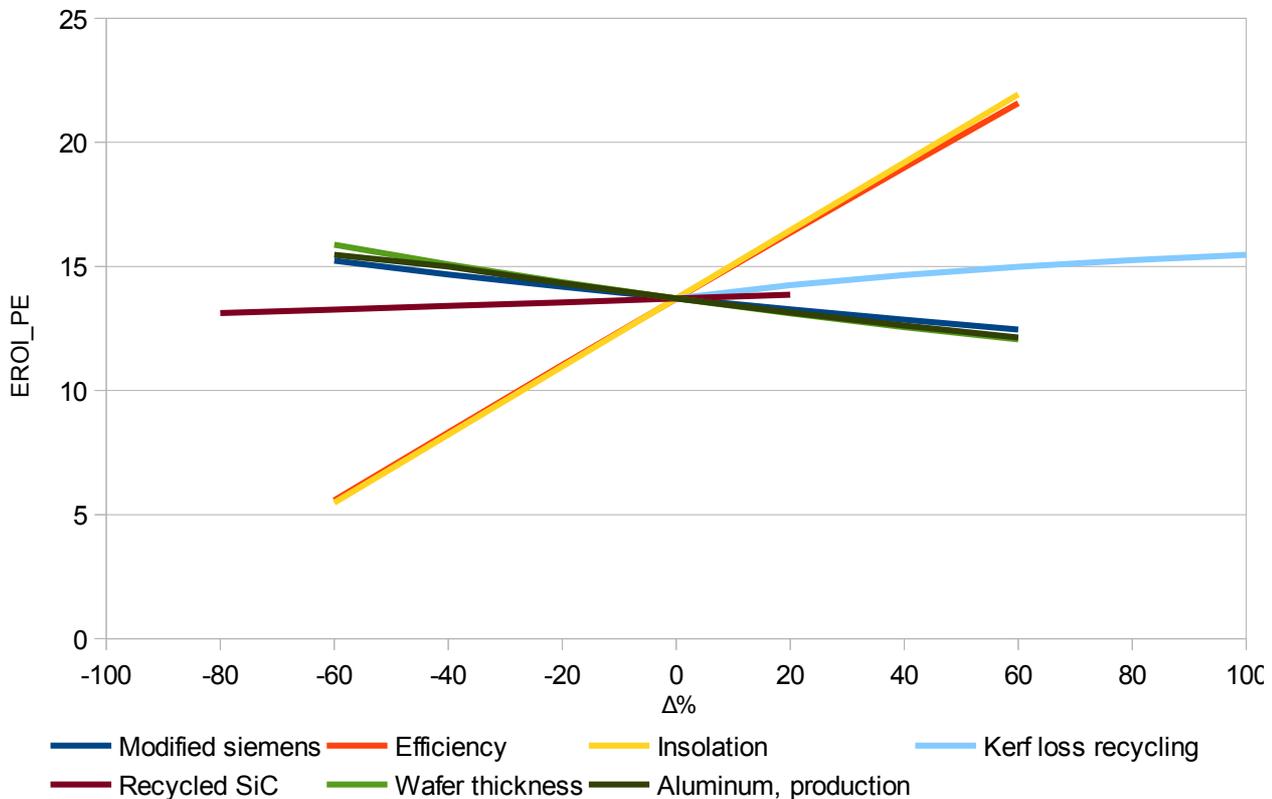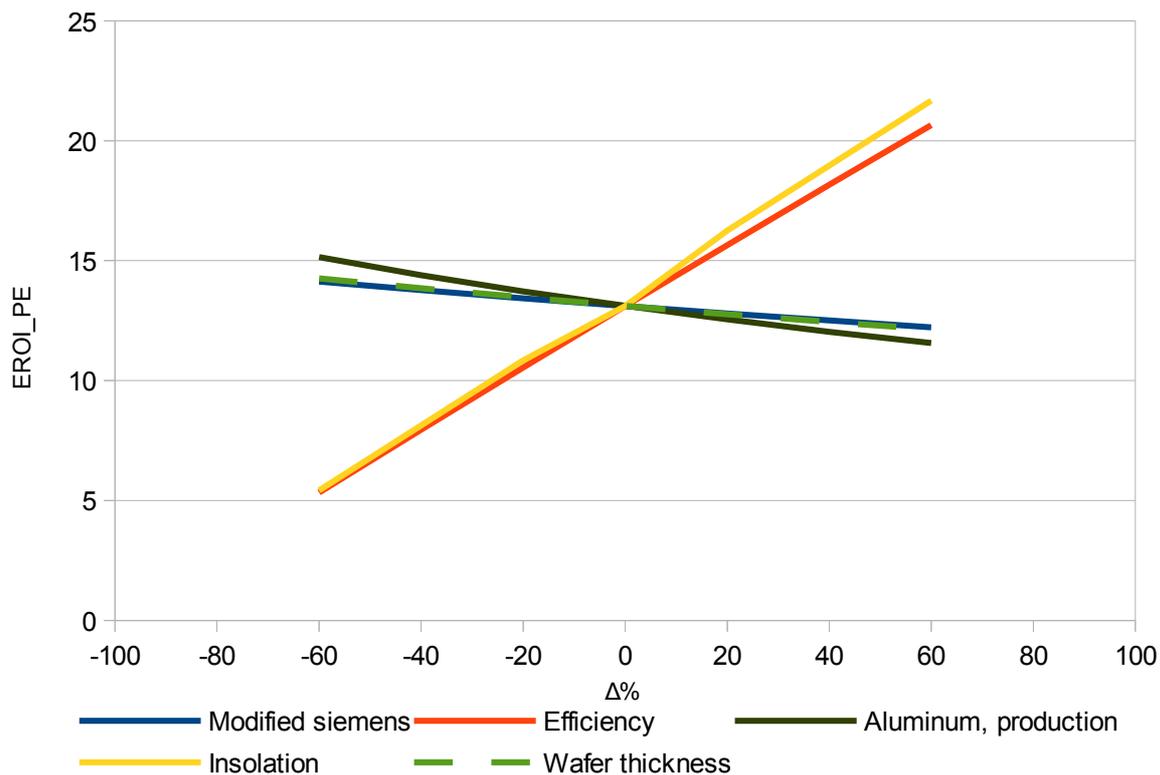

8.11 Case

Several "cases" will also be examined in order to paint a more easily understood picture illustrating the spread in possible $EROI_{PE}$ and $EROI_e$. Extended system boundaries is used (i.e total energy demand equal to that of Jungbluth et al., 2012).

8.11.1   Case 1: Worst episode ever

PV EROI show a very large variability with respect to produced energy which is dependent upon insolation. A placement which will typically result in low yields is the Stockholm region. There are plenty of building roofs and facades in such a metropolitan area, some of which are appropriate for PV installation. Mounting on slanted roof are used to model this. All three investigated panels are used, with their standard thicknesses and efficiencies. The Swedish power grid also have a large fraction of hydro- and nuclear power. Hydropower replaced by solar will not result in a larger primary energy amount returned for other use (i.e. 1:1 conversion). Nuclear power is a base load power generation system which is something PV most definitively will not replace in the near future. All production processes is assumed to take place in China (having a thermal grid efficiency comparable to UCTE). The picture is worsened even more by using "outdated" production processes resulting in comparatively thicker wafers (+20%, corresponding to 228, 240 and 300 μm for c-Si, mc-Si and r-Si respectively). Finally the extended system boundaries are added, so the system size is equivalent to Jungbluth et al..

Table 8.13: Case 1 EROI

	EROI$_{PE}$	EROI$_e$	Energy demand (MJ$_{PE}$)	Production
c-Si	5.5	1.7	51970	88662
mc-Si	5.93	1.84	48223	88622
r-Si	6.11	1.89	46797	88622

8.11.2 Case 2: Dry wasteland

The sunniest regions in the world can be found in northern Africa and the Saharan desert. The climate is dry with very little clouds. Decision-makers both on the African continent and in Europe (mainly Europe) dream of transferring power produced in the desert to more populous regions. The desert is unfortunately a hostile environment and not very many buildings are available for solar module mounting. A free-standing facility must thus be constructed, which increases the BoS energy demand. Frames may be piled directly into the ground if appropriate, else a concrete foundation must be laid, concrete which is reinforced by steel. Steel (and zink) is also used for fencing since remote locations containing high-value products are prone to theft. A free-standing mounting system piled into the ground uses 3.98 kg of aluminum, 7.21 kg of steel and 1.24 kg of concrete per square meter panel. Mounting system which utilize a heavy concrete foundation (e.g. to be used for tracker support and/or ground stability) have a materials demand of 42 kg of steel and 47 kg of concrete per square meter panel area. The heavy-foundation option is assumed to support a one-axis tracking device with no embodied energy cost. The metallurgical route from MG-Si to SoG-Si is assumed, which has a lower energy demand than the conventional Siemens-process. The harsh desert environment is also assumed to increase the performance degradation rate, from 0.5 %/y to 1 %/y.

Table 8.14: Case 2 EROI, without concrete foundation

	EROI$_{PE}$	EROI$_e$	Energy demand (MJ$_{PE}$)	Production
c-Si	13.99	4.34	40830	177108
mc-Si	15.61	4.84	36604	177108
r-Si	14.95	4.63	38223	177108

Table 8.15: Case 2 EROI, with concrete foundation and single axis tracker system

	EROI$_{PE}$	EROI$_e$	Energy demand(MJ$_{PE}$)	Production
c-Si	15.12	4.69	48973	229584
mc-Si	16.46	5.10	44986	229584
r-Si	15.64	4.85	47342	229584

8.11.3 Case 3: A bright future

China is the world's largest PV producer and an emerging market regarding installed power. There is a large growth potential. Electric energy delivered per year by a solar panel in a favorable spot in Beijing is comparable to that of southern Europe along the Mediterranean. The Chinese electricity grid is highly dependent upon coal, which means that renewable electricity displace much primary energy. An optimistic future case is modeled by assuming that the efficiencies of c-Si, mc-Si and r-Si commercial laminates have reached levels of 22.9% (c-Si) and 18.2% (mc-Si and r-Si) (Green et al., 2012). Mc-Si and r-Si panels have the same efficiencies since they both utilize multicrystalline

silicon. A mature production technology for r-Si is assumed to exist, not resulting in efficiency losses. Wafer thickness for all three laminate types have also been reduced to 100 microns. The kerf loss is recycled up to 50% at no energy cost (i.e. all energy expenditure could be said to be allocated to "the other" 50% if we were to assume 100% recycling).

The laminates are mounted at optimal angle in Beijing on slanted roofs.

Table 8.16: Case 3 EROI

	$EROI_{PE}$	$EROI_e$	Energy demand (MJ_{PE})	Production
c-Si	19.4	6.01	24108	144955
mc-Si	18.86	5.85	24791	144955
r-Si	17.13	5.31	27298	144955

9 Discussion

The results indicates that certain processes is more important than others for PV EROI. Insolation and efficiency strongly affects EROI values, as do wafer thickness and associated kerf losses. Reasons for the importance of these processes and meaning in a wider perspective are examined. The impact of primary versus electric energy as output has proven to be very important and is discussed. Previous EROI studies including a new and ambitious by Prieto & Hall (2012) are also assessed.

9.1 Insolation and efficiency

These variables affects the EROI of PV more than any other. This can be explained by examining the numerator and denominator in the EROI expression. The numerator, E_{out}, refers to delivered electric energy (or primary energy replaced within the grid). Delivered electric energy is proportional to peak-hour insolation, and is essentially only dependent upon this (assuming constant ambient temperature and efficiencies not decreasing with time). EROI consequentely scales directly with insolation.

The kW_p is the fuctional unit of choice in this thesis. The efficiency of each panel type affects how much panel area is needed in order to assemble one kW_p of power. Each process within the production chain embodies energy in one m^2 of panel except for the inverter production which is directly added to CED at the kW_p-level. Efficiency directly affect the EROI denominator since it is the main driver regarding area requirement to reach one kW_p of installed power. These two variables (insolation and efficiency) thus affect the outermost "layers" of the EROI expression:

$$ EROI = \frac{P_{DC,STC} \cdot \frac{H_g}{G_{g,STC}}}{E_{CED/m^2} \cdot A + E_{inv}} \qquad (13) $$

where $P_{DC,STC}$ is rated power, $G_{g,STC}$ is irradiance under STC and H_g is insolation received. The amount of electric energy delivered is directly influenced by multiplying this variable. The area A is given by $1kW_p/\eta$ where η is the panel efficiency. Changing this efficiency directly dictates how much area is needed, and thus the size of the denominator.

It can also be seen in the graphs that changes in insolation results in a slightly steeper slope compared to efficiency changes. This is understandable since changes in efficiency (i.e. area

demand) doesn't affect the inverter energy demand, in contrast to changes in insolation which affects the complete numerator. The energy requirement for one kW_p of each panel type exceeds 20000 MJ_{PE}, and E_{inv} amounts to less than 500 MJ_{PE} which means that the inverter influence is small but still discernible. The use of simple one-axis tracking system could also help increase produced energy by approximately 30% (compare produced energy in Table 33 and Table 34).

9.2   Wafer thickness and kerf losses

Change in wafer thickness will affect the amount of silicon (mono-, multi- or ribbon-based) in each wafer. Monocrystalline wafers is sawed from monocrystalline ingots. Producing these ingots is very energy intensive, and the thinning (or thickening) of wafers means this process becomes less (or more) important. Sensitivity is thus high. Multicrystalline wafers is cut from multicrystalline ingots, which are not as energy intensive to produce. Sensitivity is still high, but not as high as for the monocrystalline wafers. The ribbon-based wafers are produced directly from SoG-Si and exhibit a much lower sensitivity compared to the other two production processes.

The calculations in this thesis regarding the effect of changing wafer thickness assumes that the kerf loss equals the weight of the wafer (i.e. 50% kerf loss). This condition could be said to model a condition where the wire diameter changes as the wafer thickness does. The thinning of wafers would under "real" conditions mean that kerf loss increases as more wafers can be produced from a given ingot length. More wafers means additional sawing wires have been used, and the ratio of wire thickness to wafer thickness will increase unless effort is made to reduce wire diameter.

Wafer thickness also affect efficiency. A thicker wafer will absorb a comparatively larger amount of sunlight than a thinner wafer. This effect can be mitigated by the use of reflective back-coatings which increase chances of photon capture while decreasing thickness. Ravi (2011) offers a short overview, claiming that maximum efficiency for crystalline silicon occurs at a thickness of approximately 50-100 μm. This could very well be an attempt to market the 50 μm crystalline wafer technology Ravi represents. Tool et al. (2002) present experimental data indicating that efficiency and thickness is independent for thickness larger than 200 μm, but thinner wafers may lead to a decrease in efficiency. The limit to sawing is said to occur at 80 μm, but breakage rates increase already at 180 μm (Ravi, 2011).

All mechanical sawing activities induce kerf losses, this can not be avoided. Recycling of this kerf loss have a relatively large impact on the EROI for the system at hand. The recycling process is assumed to require no energy in this thesis which obviously is unrealistic, but no information regarding typical energy demand has been found. The recycling of SiC, a process which essentially means removing useful SiC from consumed SiC and kerf loss particles, takes only 6.5% of the energy compared to primary production (Jungbluth et al., 2012). The energy demand for recycling kerf loss is likely higher due to smaller particle sizes, but could very well be of the same order as SiC recycling energy demand.

9.3   Siemens-process and wafer thickness

The Siemens-process is often described as the most energy-intesive process of the PV manufacturing process. It should as such prove to be quite important, and it is. One should however mention the relation to wafer thickness, which turns out to be even more important. The sawing of wafers occur *after* the Siemens-process within the process chain. Amount of energy embodied in each wafer directly corresponds to the weight of each wafer. More energy is embodied per kilogram of silicon at the sawing stage than what is embodied after the Siemens-process (due to SoG-Si being smelted and solidified into c-Si or mc-Si ingots which further embodies energy into the product). The sensitivity slope for the Siemens-process is approximately shared for all panel types, but the

gap closes relative to wafer thickness sensitivity for mc-Si and r-Si panels. The production of mc-Si and silicon ribbons is much less energy-intensive than producing c-Si ingots through the Czochralski-process.

9.4   Previous photovoltaic EROI studies

Energy payback time (EPBT) calculations are especially numerous for photovoltaic systems throughout their history. In the beginning of photovoltaic technology there was a very real possibility that systems would not be able to repay the energy that went into production. We now know this is not true and that most systems are able to repay their energy debt, but the habit of calculating EPBT is still standard practice in many instances (Richards and Watt, 2007). The EROI can be inferred by dividing the expected lifetime of the investigated system with it's EPBT. The energy payback time was of no concern in the late sixties and early seventies, as the main use for solar panels was space applications for which there was no substitutes. The lifetime of photovoltaic cells was also largely unknown. There was an early report in 1974 citing EBPT for polycrystalline (pc-Si) cells in the range of 5.1-10.2 years depending on efficiency, and 3 years for monocrystalline (c-Si) cells. This would translate into an EROI of roughly 2-4:1 for mc-Si and 6.7:1 for c-Si assuming a 20-year lifetime for early solar cells. Some studies however cited very long EPBT in the range of 20-40 years due to low wafer yields, which corresponds to a low EROI. The payback times decreased as wafer yields increased during the seventies. Most energy payback times had shortened to below 10 years during the 1980s and 1990s, while lifetime increased. (Richards and Watt, 2007)

Alsema and Nieuwlaar (2000) states that typical polycrystalline photovoltaic systems had an EPBT of 2.5-6 years at the start of the millenium. Payback times generally increases with decreasing irradiation, and also with ground-mounting due to frame requirements. An expected lifetime of 25-30 years then yields an inferred EROI of approximately 4-12:1 depending on circumstances. Meijer et al. presented a study in 2003 which gave an EPBT of 3.5 years for mc-Si cells (Meijer et al., 2003). Assuming a 30 year lifetime yields an EROI of approximately 8.6:1.

Silicon-based photovoltaic cells was during this period primarily being manufactured from electronic-grade or off-grade silicon, which requires a lot of energy. As demand for photovoltaics increased so did the demand for a production process yielding solar-grade silicon. Such processes generally require less energy than production of electronic-grade silicon. Raugei et al. calculated EROI by dividing the expected lifetime (30 years) with EPBT and found that c-Si, mc-Si and silicon ribbon cells have an EROI of 19:1, 19:1 and 30:1 respectively. EBPT for these examined panels are less than 2 years. The authors transformed electric energy output into primary energy equivalents, something which inflates EROI compared to studies not having done so. The ribbon-based panels are found to have a much larger EROI even though panel efficiency is comparable to that of sawed wafers, which can be explained by the lower cumulative energy demand (Raugei et al., 2012).

One must exercise caution when examining EROI from previous studies, especially large meta-studies. Often no information regarding system boundaries are available, which makes comparison between results difficult. The same is true for quality corrections, electricity mix used and other system assumptions.

9.5   Short assessment of Prieto & Hall (2012)

One of the widest and most inclusive systems found by the author of this thesis is the one by Prieto and Hall (2013). Their analysis deals with the photovoltaic industry in Spain and the resulting EROI. The authors conclude that the Spanish photovoltaic industry has an $EROI_e$ of 2.45:1 when treating electric output as thermal equivalents and $EROI_{PE}$ of 7.35:1. The boundaries used is claimed

to correspond to the EROI$_{stnd}$ proposed by Murphy et al. (2011). Prieto and Hall (2013) use a somewhat different approach than most life-cycle analyses concering PV: *all* PV in Spain are assessed instead of a single panel or one kW$_p$. The installed photovoltaic power in Spain is mainly in the form of larger *plants*, not *panels* on housing roofs etc. Prieto and Hall use a generalized plant location and infrastructure (e.g. fences, roads, concrete foundations and evacuation lines) and activities connected to the operation of the plant (e.g. security, washing of panels) as the direct inputs. All other inputs are considered indirect, even the PV panels themselves. This is in stark contrast to the vast majority of life-cycle assessments for PV where one instead generally follows the path of silicon from quartz to panel area/installed power/delivered energy. Inputs are added and divided by 25 years to give the annual "cost", which is then compared to countrywide PV output in order to find the EROI. This methodology is clearly inspired by previous work by Charles Hall and his colleagues regarding fossil fuels where the annual EROI is evaluated and presented as time series.

The system boundaries are very wide, including (energy) costs of such things as insurance, fairs & exhibitions, administration and even the education of engineers. This is admirable, but at the same time claiming the calculated EROI corresponds to the boundaries of EROI$_{stnd}$ is problematic. The framework by Murphy et al. (2011) says that inclusion of "indirect labor consumption" would mean moving away from EROI$_{stnd}$. Including indirect (off-site) inputs of labor character (e.g. civil servants and utilities personnel) would, according to the author of this thesis, disqualify the analysis by Prieto and Hall from being placed in the EROI$_{stnd}$ category. The cost for these services must include the workers salary (since the income these services generate support the individuals performing the work at the very least), and hence labor consumption is included. This is not necessarily a problem, but things should be called what they really are and placing the EROI calculated by Prieto & Hall in the EROI$_{stnd}$-category is somewhat confusing.

It seems likely that Prieto's background as an PV plant manager has influenced the choice of plant location and infrastructure as the direct inputs. The attempt to place the calculated EROI within the EROI$_{stnd}$ category seems somewhat forced to the author of this thesis.

Prieto and Hall's relatively wide system boundaries can be put into perspective by examining more conventional LCA's which are process-chain based. Desideri et al. (2012) have performed a process-chain LCA for a large PV plant. The plant location and infrastructure seem to be the central unit examined, much as in Prieto and Hall (2012). The process-chain analysis performed by SimaPro in conjunction with LCI databases yields an EROI$_e$ of 4.83. This does not include the financial services accounted for by Prieto and Hall but shares many of the on-site and some off-site processes. Delivered energy is treated as electric energy, not primary energy. This is twice as high a EROI$_e$ as the value stated by Prieto & Hall.

9.6   Displaced fossil primary energy versus thermal equivalents

Electric energy delivered by the existing grid correspond to a certain amount of primary energy. A coal-fired power plant with a thermal efficiency of 30% will have used three times as much primary energy for every unit of electric energy output. The electric energy output from solar power plants is directly treated as primary energy (in accordance to IEA guidelines). This output is however at times transformed into *fossil* primary energy equivalents. The delivered electrical energy is thought of as displacing conventional electric energy.

Stoppato (2008) does not seem to convert electric energy to primary energy, while Fthenakis and Kim (2011) does. This is not a problem in the individual reports, but becomes problematic once EROI calculated with primary energy and thermal equivalent outputs is compared to each other. The picture does not become clearer by the fact that EROI can vary wildly with system boundaries as well. Good thing is that the IEA LCA guidelines for PV at least specifies that it should be stated

whether or not output is converted to primary energy (Alsema et al., 2009). Unfortunately, as has been shown by Stoppato, this is not always clear, only implied.

Converting the delivered PV electric energy into primary energy equivalents by using the thermal grid efficiency enables comparison with other energy producing system (e.g. production of oil). This essentially implies that PV electric energy *replace* fossil fuels. Fossil fuel is then assumed to be saved or available for use elsewhere. One can however not be sure that renewable electric energy will replace fossil fuels under the current regime of growing electric energy use. Growth rates for renewable electric energy would have to outpace growing demand for this to occur. This is especially problematic with existing energy systems dominated by coal and other combustible solids, since other uses but energy production is sparse. Oil and gas on the other hand can more easily be assumed to be displaced, since these energy carriers are "easily" diverted into sectors such as transportation (e.g. fuels) or agriculture (e.g. fertilizers) through refinement processes. The amount of primary energy preserved for alternative use will also diminish as the amount of flowing renewables within the electricity grid increase. If the production chain of a renewable technology in itself use a lot of renewable electric energy (e.g. hydropower) but the general thermal grid efficiency to which electric energy is fed is low then a comparatively large amount of fossil fuels are "saved". If one, like Prieto & Hall, would distribute the energy demand over the lifetime of a PV system (i.e. MJ_{PE}/y energy demand) then $EROI_{PE}$ may appear to decrease over the product lifetime due to increased renewable energy within the electricity grid. The opposite is also true, if energy demand would have been allocated to each year with larger weight during the first years of operation (i.e. in accordance to economic annuity calculations) then EROI would appear to increase as time passes.

One could also question whether or not the electric energy inputs should be converted to primary energy when output is not. There seem to be consensus that this should be done, and the author of this thesis agrees since it is known what the used electric energy input originates from and where it ends up, it is unambiguous. This is in contrast to the delivered PV electric energy; the destination is not known at the plant energy meter.

Both $EROI_e$ and $EROI_{PE}$ should always be stated next to one another in text (where possible/data exists), as no ambiguity will exist and the reader will instantaneously know that the author have considered both accounting possibilities.

EROI of fossil fuels will almost always have primary energy/heating values in the numerator, which makes comparison with the EROI for PV impossible if output is presented as straight electric energy units. A more appropriate comparison would in that case be the EROI regarding coal-powered electric energy generation and PV. Discrediting the relatively low EROI of PV by comparison to the higher values of fossil fuels is somewhat unfair, as PV delivers electric energy directly into the grid. There is a world of difference between oil (or even gasoline) and electric energy. This problem can be mitigated through the use of quality correction, but such corrections are often only described in general terms or simply "given". For example: the author of this thesis have yet to come by a clear step-by-step instruction for Divisia-correction. What's more is that such Divisia-corrections seem to be used mostly a tool for examining the relationship between energy use and GDP.

10 Conclusion

Case 1-3 all use the same system boundaries but different assumptions (deemed realistic by the author of this thesis). $EROI_{PE}$ and $EROI_e$ are approximately three times as large in case 3 compared to case 1. Assumptions obviously play a huge role regarding EROI, and this is not even including differing system boundary size. One of the main conclusions is thus that presenting a single EROI

value is, at least for PV systems, not very enlightening. Some authors unfortunately do exactly this. Furthermore the difference between output in primary energy units and thermal equivalents is incredibly important and researchers need to be very clear about this.

The main drivers for EROI are insolation/energy produced and panel efficiency. Efficient panels translates into less area needed for a given nominal power rating. Panels available commercially today is not as efficient as the best cells under laboratory conditions by a long shot, and improving efficiency in commercial panels are key. Tracking systems can be of utmost importance, and a push towards low-weight one-axis tracking systems could increase produced energy by ~30%, translating into an EROI-increase of ~8% (see case 2).

The Siemens-process is often mentioned as one of the most energy-intensive steps when producing solar cells. This study however has shown that the Czochralski-process is even more energy-demanding per produced mass. The results show that mc-Si and r-Si panels are more sensitive to energy demand changes when producing SoG-Si ($\Delta EROI_{PE}$/% of 0.061 and 0.044 respectively) than c-Si panels ($\Delta EROI_{PE}$/% of 0.038) using the reduced system boundaries. Casting mc-Si ingots and ribbons are nowhere near as demanding as the Czchoralski-process, so the relative importance of the Siemens-process is larger for these two panel types.

The author also conclude that the thinning of wafers, preferably through new production techniques is of importance. Especially c-Si panels ($\Delta EROI_{PE}$/% of 0.095, reduced system) are sensitive to wafer thickness due to both Siemens- and Czochralski-processes being necessary for production. Technologies which produce wafers without sawing will obviously be very important for increasing photovoltaic EROI.

Kerf-loss recycling is as of 2013 not commercially implemented. A rather large material (and hence embodied energy) reduction can be made if this technology is implemented. Assuming that an energy demand level of one tenth of primary production is realistic for a mature kerf loss recycling technology would mean that the *reduced system* $EROI_{PE}$ would increase from 20:1 and 24:1 to approximately 26:1 and 29:1 for c-Si and mc-Si respectively. The author of this thesis concludes that this is an important field of further study and that initial energetic marginal returns for introducing such technology could be large.

Work aiming to reduce the silicon- or energy demand for panel production should focus on downstream processes, as reduced amount of silicon in a complete panel means less material overall across the board.

$EROI_{PE}$ of photovoltaics in Case 2 & 3 are above the "threshold" of 8:1 (as shown in illustration 5, net energy cliff), meaning higher- or lower $EROI_{PE}$ will not result in a significant marginal increase- or decrease of net energy. The author concludes that the $EROI_{PE}$ of photovoltaics, at least using the system boundaries in this thesis, are "good enough" and does not place overly tight constraints on economic growth according to the net energy cliff concept.

11   References

Aberle, A.G., 2009. Thin-film solar cells. Thin Solid Films 517, 4706–4710.

Alsema, E., Frischknecht, R., Fthenakis, V., Held, M., Chul Kim, H., Pölz, W., Raugei, M., de Wild Scholten, M., 2009. Methodology Guidelines on Life Cycle Assessment of Photovoltaic Electricity (No. IEA-PVPS T12-01:2009). IEA - PVPS.

Alsema, E.., Nieuwlaar, E., 2000. Energy viability of photovoltaic systems. Energy Policy 28, 999–1010.

Bazilian, M., Onyeji, I., Liebreich, M., MacGill, I., Chase, J., Shah, J., Gielen, D., Arent, D., Landfear, D., Zhengrong, S., 2013. Re-considering the economics of photovoltaic power. Renewable Energy 53, 329–338.

Breyer, C., Gerlach, A., 2013. Global overview on grid-parity. Progress in Photovoltaics: Research and Applications 21, 121–136.

Brown, M.T., 2004. A picture is worth a thousand words: energy systems language and simulation. Ecological Modelling 178, 83–100.

Bullard, C.W., Penner, P.S., Pilati, D.A., 1978. Net energy analysis: Handbook for combining process and input-output analysis. Resources and Energy 1, 267–313.

Cahalan, R., n.d. Solar Radiation [WWW Document]. URL http://atmospheres.gsfc.nasa.gov/climate/index.php?section=136 (accessed 11.29.12).

Chandler, D.L., 2010. Explained: Bandgap - MIT News Office [WWW Document]. MIT's News Office. URL http://web.mit.edu/newsoffice/2010/explained-bandgap-0723.html (accessed 11.26.12).

Chen, G.Q., Yang, Q., Zhao, Y.H., 2011. Renewability of wind power in China: A case study of nonrenewable energy cost and greenhouse gas emission by a plant in Guangxi. Renewable and Sustainable Energy Reviews 15, 2322–2329.

Chiou-Wei, S.Z., Chen, C.-F., Zhu, Z., 2008. Economic growth and energy consumption revisited — Evidence from linear and nonlinear Granger causality. Energy Economics 30, 3063–3076.

Cleveland, C.J., 1992. Energy quality and energy surplus in the extraction of fossil fuels in the U.S. Ecological Economics 6, 139–162.

Cleveland, C.J., O'Connor, P.A., 2011. Energy Return on Investment (EROI) of Oil Shale. Sustainability 3, 2307–2322.

Corkish, R., 2006. Solar Cells. Encyclopedia of Energy.

Derbouz, A., Slaoui, A., Jolivet, E., de Moro, F., Belouet, C., 2012. N-type silicon RST ribbon solar cells. Solar Energy Materials and Solar Cells 107, 212–218.

Desideri, U., Proietti, S., Zepparelli, F., Sdringola, P., Bini, S., 2012. Life Cycle Assessment of a ground-mounted 1778 kWp photovoltaic plant and comparison with traditional energy production systems. Applied Energy 97, 930–943.

EAA, 2008. Environmental Profile Report for the European Aluminum Industry (LCA).

Filtvedt, W.O., Javidi, M., Holt, A., Melaaen, M.C., Marstein, E., Tathgar, H., Ramachandran, P.A., 2010. Development of fluidized bed reactors for silicon production. Solar Energy Materials and Solar Cells 94, 1980–1995.

Frankl, P., Nowak, S., 2012. Technology Roadmap: Solar photovoltaic energy (Roadmap). IEA - PVPS.

Fraunhofer ISE, 2011. Scientists in Freiburg Optimize Efficiency and Costs of PV Modules - New Technology Center at Fraunhofer ISE Builds Bridge to PV Industry — Fraunhofer ISE. URL http://www.ise.fraunhofer.de/en/press-and-media/press-releases/press-releases-2011/scientists-in-freiburg-optimize-efficiency-and-costs-of-pv-modules-new-technology-center-at-fraunhofer-ise-builds-bridge-to-pv-industry (accessed 12.12.12).

Frischknecht, R., Jungbluth, N., Althaus, H.-J., Doka, G., Heck, T., 2007. ecoinvent report no. 1:

Overview and Methodology.

Fthenakis, V.M., Kim, H.C., 2011. Photovoltaics: Life-cycle analyses. Solar Energy 85, 1609–1628.

Gagnon, L., Bélanger, C., Uchiyama, Y., 2002. Life-cycle assessment of electricity generation options: The status of research in year 2001. Energy Policy 30, 1267–1278.

Gagnon, N., Hall, C.A.S., Brinker, L., 2009. A Preliminary Investigation of Energy Return on Energy Investment for Global Oil and Gas Production. Energies 2009, 490–503.

Glockner, R., Odden, J.-O., Halvorsen, G., Tronstad, R., de Wild-Scholten, M., 2008. Environmenta life cycle assessment of the Elkem Solar metallurgical process route to solar grade silicon with focus on energy consumption and greenhouse gas emissions (No. m08069), Silicon for the Chemical and Solar Industry IX.

Green, M.A., Emery, K., Hishikawa, Y., Warta, W., Dunlop, E.D., 2012. Solar cell efficiency tables (version 39). Progress in Photovoltaics: Research and Applications 20, 12–20.

Guilford, M.C., Hall, C.A.S., Connor, P.O., Cleveland, C.J., 2011. A New Long Term Assessment of Energy Return on Investment (EROI) for U.S. Oil and Gas Discovery and Production. Sustainability 3, 1866–1887.

Gupta, A.K., Hall, C.A.S., 2011. A Review of the Past and Current State of EROI Data. Sustainability 3, 1796–1809.

Hall, C.A.S., 2008. The Oil Drum: Net Energy | Unconventional Oil: Tar Sands and Shale Oil - EROI on the Web, Part 3 of 6 [WWW Document]. URL http://www.theoildrum.com/node/3839 (accessed 10.25.12).

Hall, C.A.S., Balogh, S., Murphy, D.J.R., 2009. What is the Minimum EROI that a Sustainable Society Must Have? Energies 2, 25–47.

Hall, C.A.S., Dale, B.E., Pimentel, D., 2011. Seeking to Understand the Reasons for Different Energy Return on Investment (EROI) Estimates for Biofuels. Sustainability 3, 2413–2432.

Hall, C.A.S., Klitgaard, K.A., 2012. Energy and the Wealth of Nations, 1st ed.

Herendeen, R.A., 2004. Net Energy Analysis: Concepts and Methods. Encyclopedia of Energy.

Hersch, P., Zweibel, K., 1982. Basic Photovoltaic Principles and Methods. Technical Information Office.

IEA, 2012. Energy Balances of OECD Countries 2012. Organisation for Economic Co-operation and Development, Paris.

IEA, OECD, eurostat, 2005. Energy Statistics Manual (Statistics manual).

IEA PVPS Task 1, 2012. Trends in Photovoltaic Applications: Survey report of selected IEA countries between 1992 and 2011 (No. T1-21:2012). IEA - PVPS.

Johnson, J., Reck, B.K., Wang, T., Graedel, T.E., 2008. The energy benefit of stainless steel recycling. Energy Policy 36, 181–192.

Jordan, D.C., Kurtz, S.R., 2013. Photovoltaic Degradation Rates—an Analytical Review. Progress in Photovoltaics: Research and Applications 21, 12–29.

JRC, 2012. PV potential estimation utility [WWW Document]. URL http://re.jrc.ec.europa.eu/pvgis/apps4/pvest.php (accessed 12.4.12).

Jungbluth, N., Stucki, M., Flury, K., Frischknecht, R., Büsser, S., 2012. Life Cycle Inventories of Photovoltaics (LCI).

Kim, D.S., Yelundur, V., Nakayashiki, K., Rounsaville, B., Meemongkolkiat, V., Gabor, A.M., Rohatgi, A., 2006. Ribbon Si solar cells with efficiencies over 18% by hydrogenation of defects. Solar Energy Materials and Solar Cells 90, 1227–1240.

Kubiszewski, I., Cleveland, C.J., Endres, P.K., 2010. Meta-analysis of net energy return for wind power systems. Renewable Energy 35, 218–225.

Luque, A., Hegedus, S., 2011. Handbook of Photovoltaic Science and Engineering. John Wiley & Sons.

Meijer, A., Huijbregts, M. a. J., Schermer, J.J., Reijnders, L., 2003. Life-cycle assessment of photovoltaic modules: Comparison of mc-Si, InGaP and InGaP/mc-Si solar modules.

Progress in Photovoltaics: Research and Applications 11, 275–287.

Mulder, K., Hagens, N.J., 2008. Energy Return on Investment: Toward a Consistent Framework. AMBIO: A Journal of the Human Environment 37, 74–79.

Murphy, D., 2009. The Oil Drum: Net Energy | EROI Update: Preliminary Results using Toe-to-Heel Air Injection [WWW Document]. URL http://netenergy.theoildrum.com/node/5183 (accessed 10.25.12).

Murphy, D.J., Hall, C.A.S., Dale, M., Cleveland, C., 2011. Order from Chaos: A Preliminary Protocol for Determining the EROI of Fuels. Sustainability 3, 1888–1907.

Müller, A., Ghosh, M., Sonnenschein, R., Woditsch, P., 2006. Silicon for photovoltaic applications. Materials Science and Engineering: B 134, 257–262.

Norgate, T.E., Jahanshahi, S., Rankin, W.J., 2007. Assessing the environmental impact of metal production processes. Journal of Cleaner Production 15, 838–848.

NREL, 2012. PVWATTS v. 1 [WWW Document]. URL http://rredc.nrel.gov/solar/calculators/pvwatts/version1/ (accessed 12.4.12).

Odum, H.T., 1973. Energy, Ecology, and Economics. Ambio 2, 220–227.

Peet, J., 2004. Economic Systems and Energy, Conceptual Overview, in: Cutler J. Cleveland (Ed.), Encyclopedia of Energy. Elsevier, New York, pp. 103–115.

petroleum :: Status of the world oil supply -- Britannica Online Encyclopedia [WWW Document], n.d. URL http://www.britannica.com/EBchecked/topic/454269/petroleum/50722/Status-of-the-world-oil-supply (accessed 1.2.13).

Polverini, D., Field, M., Dunlop, E., Zaaiman, W., 2012. Polycrystalline silicon PV modules performance and degradation over 20 years. Progress in Photovoltaics: Research and Applications n/a–n/a.

Prieto, P.A., Hall, C.A.S., 2013. Spain's Photovoltaic Revolution: The Energy Return on Investment, SpringerBriefs in Energy. Springer.

Raugei, M., Fullana-i-Palmer, P., Fthenakis, V., 2012. The energy return on energy investment (EROI) of photovoltaics: Methodology and comparisons with fossil fuel life cycles. Energy Policy 45, 576–582.

Ravi, K.V., 2011. Thin Is In, But Not Too Thin!

Rebitzer, G., Ekvall, T., Frischknecht, R., Hunkeler, D., Norris, G., Rydberg, T., Schmidt, W.-P., Suh, S., Weidema, B.P., Pennington, D.W., 2004. Life cycle assessment: Part 1: Framework, goal and scope definition, inventory analysis, and applications. Environment International 30, 701–720.

Richards, B.S., Watt, M.E., 2007. Permanently dispelling a myth of photovoltaics via the adoption of a new net energy indicator. Renewable and Sustainable Energy Reviews 11, 162–172.

Rosen, M.A., 2004. Exergy Analysis of Energy Systems. Encyclopedia of Energy.

Schönecker, A., Geerligs, L.J., Müller, A., 2003. Casting Technologies for Solar Silicon Wafers: Block Casting and Ribbon-Growth on Substrate (Internal report). ECN.

Shockley, W., Queisser, H.J., 1961. Detailed Balance Limit of Efficiency of p-n Junction Solar Cells. Journal of Applied Physics 32, 510–519.

Stackhouse, P.W., 2012. Surface meteorology and Solar Energy [WWW Document]. URL http://eosweb.larc.nasa.gov/sse/ (accessed 11.30.12).

Stern, D.I., 2011. The role of energy in economic growth. Annals of the New York Academy of Sciences 1219, 26–51.

Stoppato, A., 2008. Life cycle assessment of photovoltaic electricity generation. Energy 33, 224–232.

Tool, C.J.J., Burgers, A.R., Manshanden, P., Weeber, A.W., van Straaten, B.H.M., 2002. Influence of wafer thickness on the performance of multicrystalline Si solar cells: an experimental study. Progress in Photovoltaics: Research and Applications 10, 279–291.

Usbeck Carrillo, V., Pflieger, J., Sun, T., 2010. Life Cycle Assessment of Float Glass. PE

International.

Wang, T.Y., Lin, Y.C., Tai, C.Y., Fei, C.C., Tseng, M.Y., Lan, C.W., 2009. Recovery of silicon from kerf loss slurry waste for photovoltaic applications. Progress in Photovoltaics: Research and Applications 17, 155–163.

Warr, B.S., Ayres, R.U., 2010. Evidence of causality between the quantity and quality of energy consumption and economic growth. Energy 35, 1688–1693.

Von Blottnitz, H., Curran, M.A., 2007. A review of assessments conducted on bio-ethanol as a transportation fuel from a net energy, greenhouse gas, and environmental life cycle perspective. Journal of Cleaner Production 15, 607–619.

Xakalashe, B.S., Tangstad, M., 2011. Silicon processing: from quartz to crystalline silicon solar cells. Southern African Institute of Mining and Metallurgy, Johannesburg, Southern African Pyrometallurgy 2011.
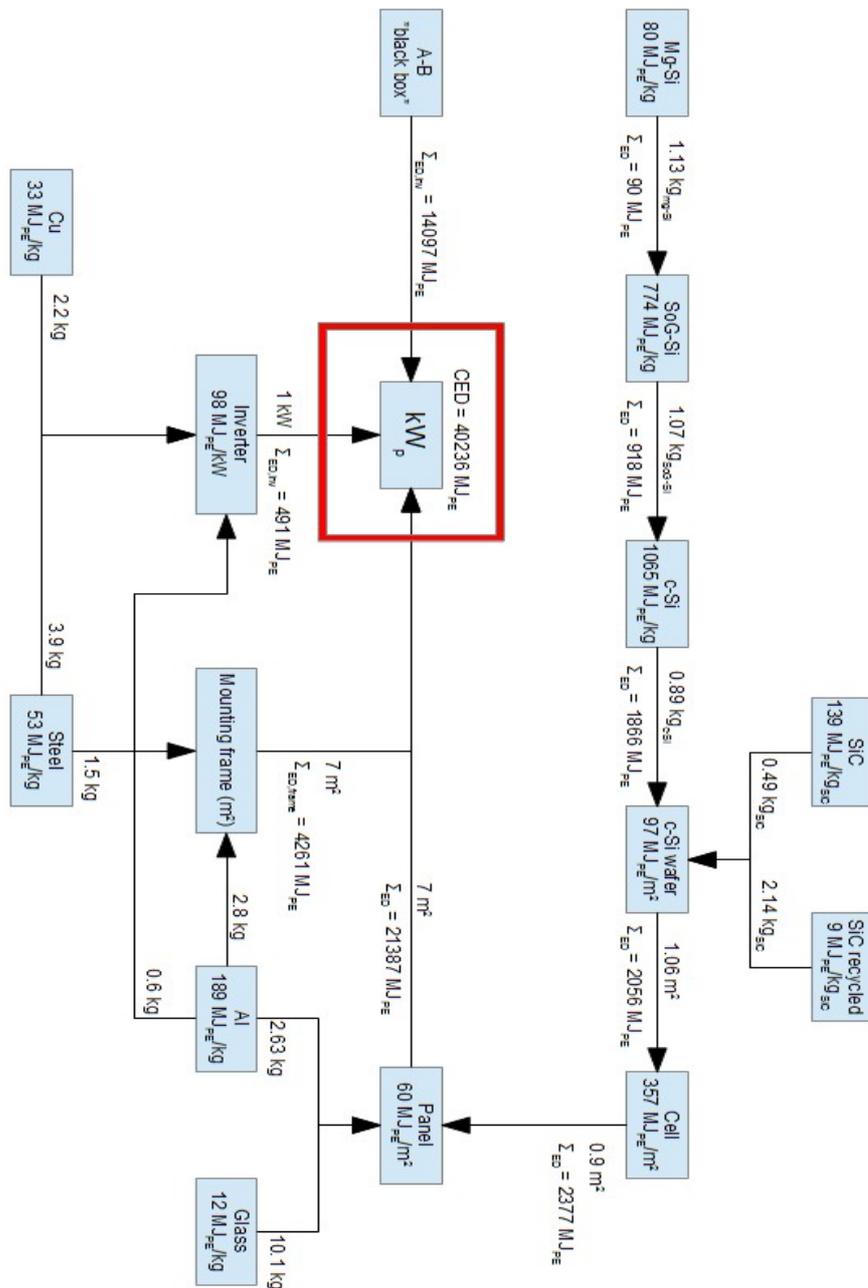
Appendix A: Calculating CED

Illustration 18: Example of CED calculation for c-Si panels. Embodied energy shown at flows after each process in the main silicon chain. Energy demand in boxes are the demand for the actual process (e.g. electric energy for machines, heat). Increasing amounts of energy is embodied after each process-step.
Example: 1.07 kg of SoG-Si turned into 0.89 kg of c-Si: 918 + (1065*0.89) = 1866 MJ$_{PE}$.
0.89 kg of c-Si ingot turned into 1.06 m² wafer including embodied energy for SiC:
1866+(97+(139*0.49)+(9*2.14))*1.06 = 2056 MJ$_{PE}$.

Appendix B: Alternative energy analysis indicators

There are other indicators except EROI within the discourse of energy analysis and net energy analysis that need some coverage. They are often interconnected with EROI but with restricted or relaxed inputs boundaries. Authors sometimes use the EROI ratio under a different flag or vice versa. An example is the *incremental energy ratio* (IER) mentioned in *Encyclopedia of Energy*, which is the gross energy output over energy input from society (Herendeen, 2004). Richards and Watt (2007) proposes what they call *energy yield ratio* (EYR) for photovoltaics, which also consists of lifetime gross energy output over energy input. This is essentially identical to EROI for PV.

Murphy et al. (2011) presents some different indicators in a short summary:

- Net energy yield ratio, NEYR:

$$NEYR = \frac{E_g - E_{in}}{E_{in}} = \frac{E_g - E_c + E_{op} + E_d}{E_c + E_{op} + E_d} = EROI - 1 \qquad (14)$$

  This shows the amount of net energy returned to society per energy unit invested.

- Fossil energy ratio, FER: $FER = \frac{E_g}{E_{ff,in}}$ $\qquad (15)$

  FER is essentially the same ratio as EROI, but with only fossil fuel inputs. This ratio is often used in conjunction with energy analysis of biofuels, as it shows how much fossil fuel that can be replaced.

- External energy ratio, EER: $EER = \frac{E_g}{E_{ext\,in}}$ $\qquad (16)$

  This ratio only takes external energy inputs into consideration, meaning that internal use of the energy resource base is disregarded. Primarily used when dealing with unconventional oil resources that use resource feedstock in situ or in an unrefined state at site.

- Energy payback time, EPBT: $EPBT = \frac{E_{in}}{E_{g,yr}}$ $\qquad (17)$

  E_{in} is the energy requirement for the system, and $E_{g,yr}$ is the annual gross energy production. EPBT indicates how long it takes for a certain system to produce as much gross energy as was expended during construction. This indicator is used especially when dealing with those renewable energy systems that have very low energy requirements during the operational phase compared to construction phase.

Appendix C: Previous EROI studies

Most explicit EROI studies have dealt with the production of petroleum products or biomass-based fuels. This is understandable in light of the purpose of net energy analysis in the US during the 1970s. The oil crises spurred an interest in substitutes for conventional imported oil, and these substitutes would need to bring some net energy gain to be useful.

EROI for oil and gas production have declined steadily since the first barrel and cubic meter were produced. The EROI for production of petroleum in the US have declined over the past 50 years, from 24:1 in 1954 to 11:1 in 2007 according to Guilford et al.. EROI for discovered oil during the past 100 years have declined extremely sharply, from over 1000:1 at the start of the twentieth century to just 5:1. This can be seen as an indicator that much less oil is being found compared to drilling effort. Increased drilling effort is also found to negatively influence EROI (Guilford et al., 2011)

A study of the global EROI for oil and gas found similar results, declining EROI over time and declining with increased drilling effort. Global estimates shows that EROI was approximately 26:1 in 1992, increasing to 33:1 at the turn of the millennium and thereafter decreasing to 18:1 in 2006. Worldwide data is incomplete compared to US data. (Gagnon et al., 2009). Interest in unconventional oil sources increased as the oil shocks of the seventies reverberated throughout the world (and primarily the US).

Hall & Murphy (2008) investigates the EROI of these energy sources in a series of online articles at The Oil Drum. Tar sands is estimated to have an EROI of 5.8-5.2:1 depending on the energy inputs included in the analysis. A meta-study in the same article shows an EROI between 1-7.2:1 (Hall, 2008). Murphy (2009) presents an EROI of 3.3-56:1 for the toe-heel air injection oil sands production process, the large variability depending on what inputs are accounted for. Cleveland and O'Connor (2011) performed a meta-study for the EROI of oil shale which shows an energy return on energy investment between roughly 2-15:1 depending in which technique is being considered. If the internal energy use is counted as an energy input, as done by Brandt, the EROI drops down to approximately 1.1-1.8:1.

Coal has a more favorable EROI than oil and gas as depletion has not yet taken it's toll. Available EROI calculations is more scarce though. Estimates by Gupta and Hall (2011) report an EROI of 30:1 between 1930-60, whereas EROI increased somewhat to 35:1, only to decline during the 1970s to 20:1. Cleveland (1992) reported a similar pattern, although with much larger values due to different accounting methods. His results indicated an EROI for thermal equivalents of 80:1 by the middle of the twentieth century, which increased to 100:1 by 1970, from where it decline to approximately 80:1 by 1984. However, if using economic quality correction the EROI drops down to roughly 20:1 across the whole investigated period.

The study of corn-based ethanol production systems have been a hot topic within the field of net energy analysis. There have been some controversy regarding whether or not ethanol is a net energy source- or sink. Hall, Dale & Pimentel performed a meta-study on two existing studies which found that EROI for corn-based ethanol varied between 0.82-1.73:1 and 0.72-17.8:1 for cellulose-based ethanol (Hall et al., 2011). A meta-study by von Blottnitz and Curran (2007) present energy yield ratios comparing the fossil energy input to the amount of ethanol output which shows ratios of 7.9:1 for Brazilian sugar cane ethanol, 2.9:1 for British sugar beet ethanol, and 5.2:1 for British wheat straw ethanol. Often in EROI/EPR studies for ethanol only fossil fuel inputs are considered, since this is the dominating fuel that ethanol is supposed to replace.

Gupta and Hall (2011) concludes that EROI for nuclear energy is likely in the range of 5-8:1, according to a meta-study done by Hall himself. The very large size and complexity of nuclear

systems and facilities could possibly be the reason that such EROI studies are hard to come by. Gagnon et al. (2002) present an EROI of 16:1 under northeastern US conditions, with a range in literature of approximately 5-100:1.

Hydropower EROI is highly site-dependent and a definitive EROI is unlikely to exist. A study by Gagnon et al. (2002) exemplifies this, where average northeastern North-American conditions yield an EROI of 205-267:1 for reservoir and run-of-river type power plants. The ranges found in international studies does however range from an EROI of roughly 25-250:1 System boundaries and site conditions evidently have a huge impact. This study was performed in 2002, but there is according to the author of this thesis no reason to assume that site-dependency should have less impact for new power plants.

The EROI of wind- and solar power is often given implicitly as an energy payback time (EPBT), which can be transformed into EROI if the system lifetime (or projected lifetime) is known. Kubiszewski et al. (2010) investigated a large number of operational wind turbines and found an average EROI of 19.8:1 with a standard deviation of 13.7. A study performed by Chen et al. (2011) give what is called the non-renewable energy investment in energy delivered (NEIED). The inverse of this ratio is analogous to FER, from which one can conclude that the examined wind power plant in China have a EROI of roughly 21:1.

Appendix D: The photovoltaic effect

A solar cell makes use of the photovoltaic effect, hence the synonyms photovoltaic cell and photovoltaics. Incoming sunlight excites electrons within the cell material, making them mobile. An internal electric field within the cell then causes the free charge to move, creating a current. Work can then be extracted by an external load.

Chandler (2010) offers a short introductory summary of the different electron states that is relevant to the theory of photovoltaics. The outermost electrons within an atom in it's ground state is said to be within the *valence* band. These electrons may be excited by the absorption of an incoming photon, which brings them to the *conduction* band. The gap between these two energy levels is called the *bandgap*, for which there exists no possible states for the electrons to be in. Metals do in general have overlapping valence- and conduction bands, whereby insulators have very large bandgaps effectively prohibiting conductance. Semiconductors are somewhere in-between, having a bandgap that is relatively easily overcome by sunlight photons.

Corkish (2006) gives an overview of the mechanisms involved in inducing a voltage and current within a solar cell. A *hole* is created when an electron within the conductance band leaves it's original place. The absence of a negative charge relative to the surroundings can be treated as a positive charge. These negative and positive charges move along an internal electric field. The semiconductor material is *doped* (i.e. manipulated) in the manufacturing process to have one layer with an excess of electrons (n-layer) and another layer which contains an excess of holes (p-layer). An electron within the n-layer is called a *majority carrier,* and a *minority carrier* when inside the p-layer. The reverse is true for holes. The contact area between these two layers is named a *p-n junction*. The excess charge in each layer will flow into the opposite layer, creating a zone over which there is a voltage. This constitutes the internal voltage which causes electron-hole pairs created within the cell to move. Pairs in the vicinity of the junction flow due to the electric field, whereby charges further away will flow towards the junction through a diffusion process. The flow of minority carriers becoming majority carriers once the p-n junction has been crossed is what determines the induced current available for work. Minority carriers may recombine with the majority carriers along the path towards the p-n junction, resulting in heat losses or photon emittance.

Conduction electrons flow out of the cell at the n-side through a connected circuit and enters the cell at the p-side where recombination is likely to occur. The energy carried by the free electrons is extracted by loads connected to aforementioned circuit. This energy is in theory equal to the amount of energy necessary to raise the electron from the valence band to the conductance band (Hersch and Zweibel, 1982).
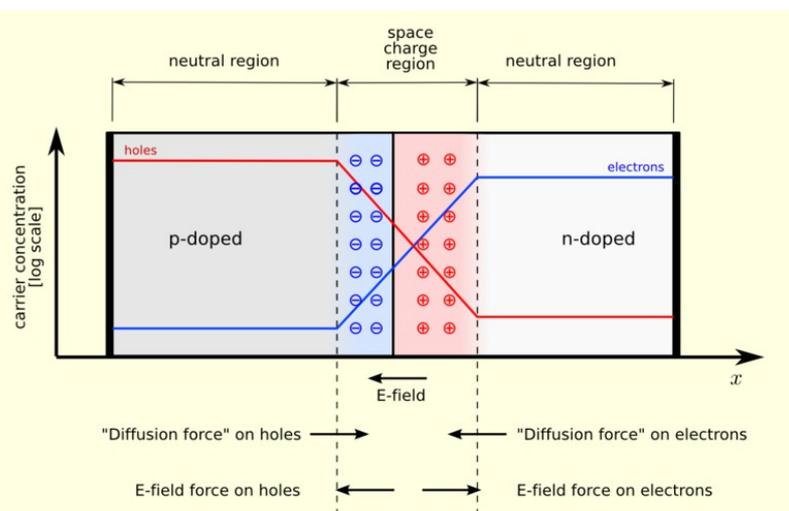

Illustration 19: p-n junction and charge distribution (Wikimedia Commons, 2007)

A theoretical limit, the Shockley-Quessier limit, for efficiency of *single p-n junction solar cells* exists much in the same way as the Betz-Lancaster limit for wind power. This puts an absolute upper limit on the amount of solar energy which can be transformed into electric energy. Developed by Shockley and Queisser (1961) the limit is also known as the *detailed balance limit* and predicts a maximum efficiency of approximately 30% for single p-n junction cells. This limit takes into account the bandgap size and recombination of electron-hole pairs. The bandgap of some materials may be too large for a portion of the incoming wavelengths (i.e. low-energy, long wavelengths), which renders these wavelengths useless for energy purposes. Too small a bandgap means that not a lot of energy was absorbed in the conductance process which equals less energy available for work in the circuit (i.e. high-energy, short wavelengths is "wasted" on a small bandgap, excess energy is lost as heat). Efficiency is further limited by recombination of electron-hole pairs (i.e. minority carriers encountering a majority carrier within a layer) which give rise to heat or photon emittance.

A photovoltaic cell with multiple junctions can be used to exceed the original Shockley-Queisser limit, although the same principles will be limiting for these cells as well. Corkish (2006) offer a short summary on this subject. Each junction is optimized according to a different wavelength, permitting higher utilization of incoming sunlight. These cells essentially consists of multiple cells made of different semiconductors with matching characteristics. Short wavelengths will be absorbed in the top layer, having a larger bandgap capable of utilizing a larger portion of the incoming energy. Layers below will utilize longer wavelengths that has too low energy for interaction with the top layer. This results in a higher theoretical Shockley-Queisser limit, but comes at the cost of very demanding and expensive manufacture. Multijunction cells is mainly used for space applications and solar energy concentrators.

Appendix E: Current market

Installed photovoltaic capacity is still a small part of global power installed but is growing, and fast that is. IEA PVPS Task 1 (2012) present an overview of the current and historical market situation regarding photvoltaics. The cumulative installed capacity in 2011 was 63.4 GW, of which 28 GW alone was installed in 2011. Germany (34.8 GW) and Italy (12.8 GW) have the largest installed capacities, followed by Japan (4.9 GW), Spain (4.3 GW), U.S. (4 GW), China (3.3 GW) and France (2.8 GW). Trends for these countries is as follows:
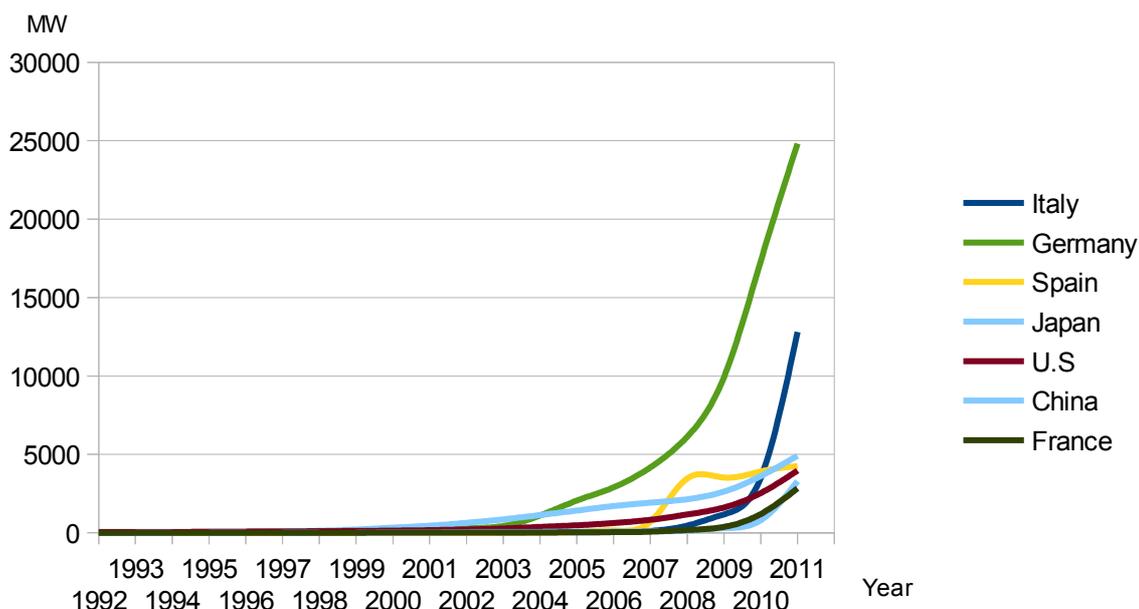
Illustration 20: Cumulative power installed in seven major PV markets (IEA PVPS Task 1, 2012)

The largest markets (i.e. experiencing the largest growth in installed power) are Italy, Germany and China with an increase of 9.3, 7.5 and 2.5 GW respectively in 2011. The development in Spain where actors rushed into the market in 2007 to get a piece of the generous feed-in tariffs, as described by Prieto and Hall (2013), can be seen. The removal of the generous subsidies has slowed down expansion considerably. Grid-connected systems absolutely dominates the market as of 2011, as do silicon wafer technologies. Total produced nameplate PV power in 2011 amounts to 33.9 GW, of which 30 GW is silicon wafer-based. It is interesting to note that manufactured nameplate power is larger than installed power (i.e. the market is currently over-producing). Manufacturing capacity is even larger, mainly due to China's sharp increase in capacity. The Chinese production capacity increased from 15 GW/yr in 2010 to 30 GW/yr in 2011.Chinese companies produce a large amount of the worlds silicon feedstock, PV cells and panels. Production capacity rose sharply during 2011 according to IEA PVPS Task 1 (2012). Production of silicon feedstock were in 2011 distributed as:
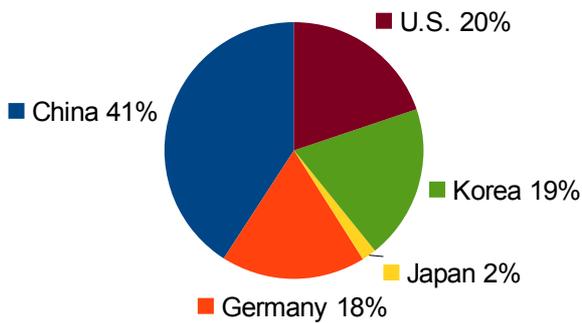
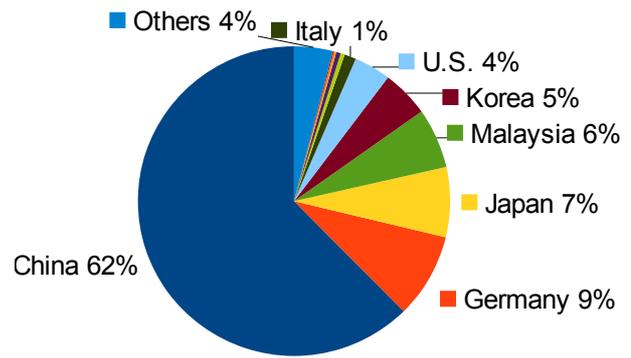*Illustration 21: Silicon feedstock major market shares*

Illustration 22: PV panel market shares by country

A similar picture emerges for panel production (as measured by power rating) in 2011; China comes out on top followed by Germany, Japan, Malaysia and Korea.

The large rise in production capacity in China have put pressure on established feedstock- and panel producers; supply outpaced demand. There is also a trend towards vertical integration within the solar power industry (IEA PVPS Task 1, 2012).

The growth of photovoltaics in the global energy system is in part driven by feed-in tariffs which are designed to attract investors into a sector which historically have had problems achieving profitability. This may however be about to change. Bazilian et al. (2013) give an overview of the development in recent years showing that average module prices have dropped from 3.5-4 $/W$_p$ in 2008 to approximately 1 $/W$_p$ in 2011 for c-Si modules. Another metric is the *levelized cost of electriciy* (LCOE) which is price per produced kWh. Whole systems are more expensive but costs continuously decrease. The same report also state that residential *grid parity* is approaching or has already been reached in some countries where electric energy prices are high. This concept is defined as the point where households make a "profit" by replacing energy bought from the grid by PV electricity without the help of subsidies or feed-in tariffs.

Breyer and Gerlach (2013) also conclude that grid parity events in the residential market is likely to occur within the next decade (2010-2020).